Title

Landmark-Free Three-dimensional Quantification of Morphological Variation and Shape Change in the Mouse Mandible: Methodological Development and Application

Author

Carlson, Chuck

Publication Date

2014

Peer reviewed|Thesis/dissertation

UNIVERSITY OF CALIFORNIA

Los Angeles

Landmark-Free Three-dimensional Quantification of Morphological Variation and Shape Change in the Mouse Mandible: Methodological Development and Application

A thesis submitted in partial satisfaction of the requirements

for the degree Master of Science in Oral Biology

by

Charles G. Carlson

2014

ABSTRACT OF THE THESIS

Landmark-Free Three-dimensional Quantification of Morphological Variation and Shape Change in the Mouse Mandible: Methodological Development and Application

by

Charles G. Carlson

Master of Science in Oral Biology

University of California, Los Angeles, 2014

Professor Won Moon, Co-chair

Professor Sotirios Tetradis, Co-chair

Objectives: Current methodologies in the field of morphometrics still employ the use of 2-dimensional images followed by a landmark-based Procrustes superimposition method to evaluate differences in shape, which can be tedious, subject to operator error, and fail to capture the true nature of shape variation between samples. The primary objective of this study is to address these limitations through the exploration and application of current methodologies used in neuroimaging and brain mapping to the field of morphometrics. By collaborating with Paul Thompson and his team at the Laboratory of Neuroimaging (LONI), we aim to:

1. Generate a 3D surface image of the mouse mandible and create an average surface for a cross sectional sample of parental strains in the Hybrid Mouse Diversity Panel (HMDP), as well as a developing longitudinal sample within a single strain.

2. Apply and modify the latest technologies used in brain mapping research to identify regional shape differences between the mandibles of these samples in 3 dimensions without the use of landmark identification, with the ultimate goal of identifying heritable quantitative traits.
3. Develop a useful, intuitive and visual method for evaluation of shape differences.

Methods: A total of fifty-three mice were studied. Ten mice, equally divided across five parental inbred strains, were obtained from the HMDP, as well as an additional 43 animals at various ages from the C57BL/6 strain. Skulls were subsequently scanned using μCT, then DICOM files transferred into a Beta version of Dolphin Imaging ® 11.7 Software. Hemi-mandibles were segmented from the entire skull and surface meshes were created using the same software. Topological correction of each hemi-mandible was performed before parametric registration and resampling of the surfaces to the same number of mesh points. Once registered to each other, a population average was then created and used as a reference template for shape comparison. Shapes were compared using the independently validated neuroimaging techniques of medial axis and tensor-based morphometrics.

Results: Population averages were created for the mandibles and four specific areas of significant shape change were identified in both the interstrain and intrastrain samples. Visual heat maps were also created to display shape differences.

Conclusions: Tensor-based morphometric evaluation of mandibular shape has far superior visualization and localization potential when compared to the current method using landmark-based analysis, while offering a more reliable solution as it eliminates the need for consistent landmark placement. Coupled with medial thickness computation, followed by

additional refinement, this methodology could potentially be applied to a variety of applications concerned with evaluating shape difference in three dimensions.

The thesis of Charles G. Carlson is approved.

Reuben Han-Kyu Kim

Sanjay Mallya

Won Moon, Committee Co-Chair

Sotirios Tetradis, Committee Co-Chair

University of California, Los Angeles

2014

TABLE OF CONTENTS

Abstract ii

List of Figures viii

Acknowledgements x

Introduction 1

Traditional Morphometrics 1

Geometric Morphometrics 4

Mouse Mandible 6

Previous Studies 7

Aims of Study 11

Materials and Methods 13

Sample Collection 14

Volume Segmentation/Surface Creation 16

Topological Correction 20

Shape Registration/Average Creation 21

Shape Comparison 24

Medial Axis 24

Principal Curvature 26

Tensor-Based Morphometrics 27

Landmark-based Procrustes 30

Results 32

Discussion 39

Limitations and Alternatives 43

Conclusions 44

References 46

LIST OF FIGURES

Figure 1 Traditional linear measurements 2

Figure 2 Undetectable differences using linear measurement 3

Figure 3 Deformation grid 4

Figure 4 Sliding semi-landmarks 5

Figure 5 Principal component/thin-plate spline analysis 6

Figure 6 Morphogenetic components of the mouse mandible 7

Figure 7 2D Procrustes landmarks for mouse mandible 8

Figure 8 Additional 2D procrustes landmarks 9

Figure 9 2D & 3D Procrustes landmarks for mouse & baboon 10

Figure 10 3D Landmarks of mouse skull 11

Figure 11 Technical Methods Workflow 14

Figure 12 Five Classical Inbred Strains 15

Figure 13 Longitudinal Sample (C57BL/6) 16

Figure 14 Mandibular Segmentation 17

Figure 15 Threshold Determination/Surface Creation 18

Figure 16 Surface Mesh Example 19

Figure 17 Spherical Mesh Representation 21

Figure 18 Sample Guassian Curvature Map 23

Figure 19 Population Average Mandible 23

Figure 20 Medial Axis Construction 25

Figure 21 Medial Axis Alignment 25

Figure 22 Sample heat map 26

Figure 23 Principal Curvature Map 27

Figure 24 Principal Component Map Sample 29

Figure 25 Interstrain Procrustes Landmarks 30

Figure 26 LONI Pipeline 32

Figure 27 Interstrain Medial Axis Results 33

Figure 28 Medial Axis Validation 34
Figure 29 Interstrain TBM Results 35
Figure 30 Interstrain PCA using TBM 36
Figure 31 Principal Component Scatter Plot (PC2 vs PC3) 37
Figure 32 Intrastrain TBM Results 38
Figure 33 Comparison of Results 39
Figure 34 Areas of Interest for RNA Extraction 42
Figure 35 Gel Electrophoresis & RIN Values 42

Acknowledgements:

I would like to thank Dr. Won Moon and Dr. Sotirios Tetradis for their unparalleled mentorship and patience, without whom this project would not have progressed to where it is today. Additionally, I offer a special thanks to Boris Gutman for his mathematical prowess and superior knowledge of neuroimaging methodologies. Boris was the backbone of most of the technical ideas and methodologies set forth in this manuscript. Further gratuity is extended to Dr. Ehab Bar and Kyle Yamamoto for their assistance in data acquisition. Finally, thank you my wife and daughter for putting up with me through this process.

Introduction:

The desire to compare the anatomical features of organisms has been central to biology for centuries. As such, shape analysis has been a fundamental part of a considerable amount of biological research.[1] The turn of last century ushered in a transition of biology from a largely descriptive field of study to a more quantitative science, and morphological studies were no exception. Studies began to include quantitative data for one or more quantifiable traits that were often summarized as mean values for comparison between groups.[2] Around the same time there were advances in statistical methods, including development of the Pearson correlation coefficient, principal component analysis and analysis of variance. By mid-century, the marriage of the two, quantitative description of morphologic shape and new statistical methods for evaluation and comparison, led to a more sophisticated analysis of these types of data; the field of modern morphometrics was born.[1]

A. Traditional Morphometrics

The term morphometric comes from the Greek words "μορφή", meaning "shape", and "μετρώ" meaning "measurement".[3] In traditional morphometrics, the approach to comparison of different shapes usually involves the use of linear distance measurements, and occasionally ratios and angular measurements are included. (Figure 1). These measurements are then analyzed using multivariate statistics, the basis of which is formed on the mathematical discoveries of Pearson, Fisher, and others. Analyses typically used in traditional morphometrics include factor analysis, Principal Component Analysis (PCA), Canonical Variates Analysis (CVA), discriminant function analysis, and multivariate analysis of variance. The former two

constituting “exploratory analyses” to identify and summarize patterns of variation within the data and the latter four to validate those patterns.[1,3]

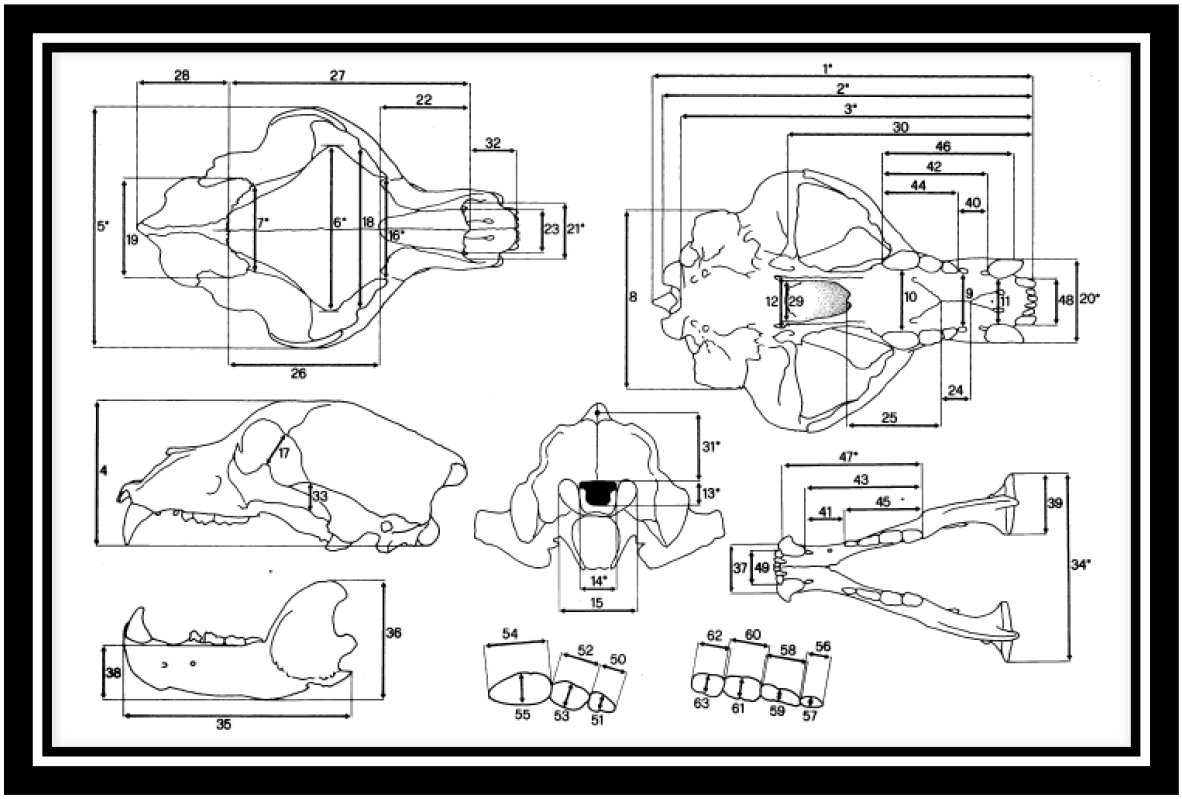

Figure 1: (From Loy et al, 2008) Traditional linear measurements as recorded from a brown bear skull.

The computation of multiple interlandmark distances in traditional morphometric analysis is also completed without accounting for the geometric configuration of the landmarks.[4] Because of this, linear measurements can often fail to detect differences in shape (Figure 2). Linear measurements also generally have a high correlation to size, and as a result there is considerable effort to develop methods for size correction, in order to identify and evaluate size-free variations in shape.[5]

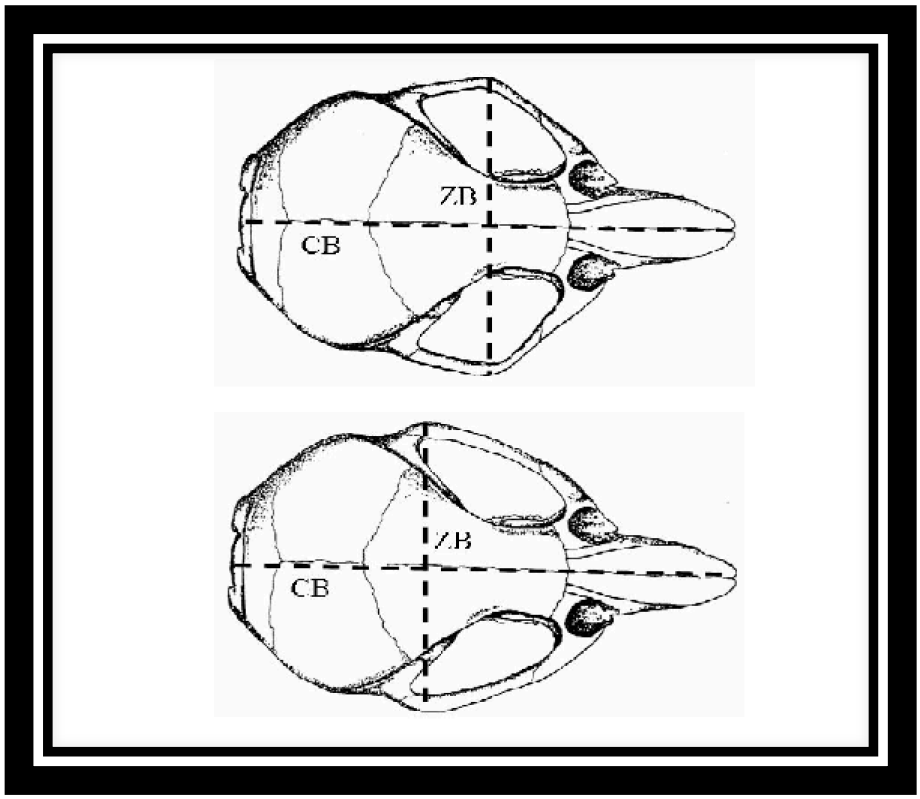

Figure 2: (From Loy et al, 2008) Shape differences not detectable with linear measurements. As illustrated by Marco Corti.

This proved to be difficult as there was no consensus on which method to use, and many of the approaches offered different interpretations of the same data. These difficulties led researchers to pursue and discover alternative ways of quantitatively analyzing morphological shapes.[1] The new morphometric toolbox combined multivariate statistics, with non-Euclidian geometry and computer aided imagery leading to what Rohlf and Marcus claimed to be the "morphometric revolution" in the early 1990s.[3,6]

B. Geometric Morphometrics

One of the inherent problems with traditional morphometrics is that the geometry of the original shape tended to get lost in the analysis; a problem geometric morphometricians sought to resolve. In fact, visualization of shape change, as well as the differences between two or more shapes, is fundamentally inherent to geometric morphometrics. This is actually one of the primary advantages of geometric morphometrics over the traditional methods; that such differences can be visualized either directly as illustrations or computer-generated images, such as deformation grids, sliding semilandmarks, warped thin-plate spline images, color maps, etc.[1,7] (Figure 3, Figure 4, Figure 5)

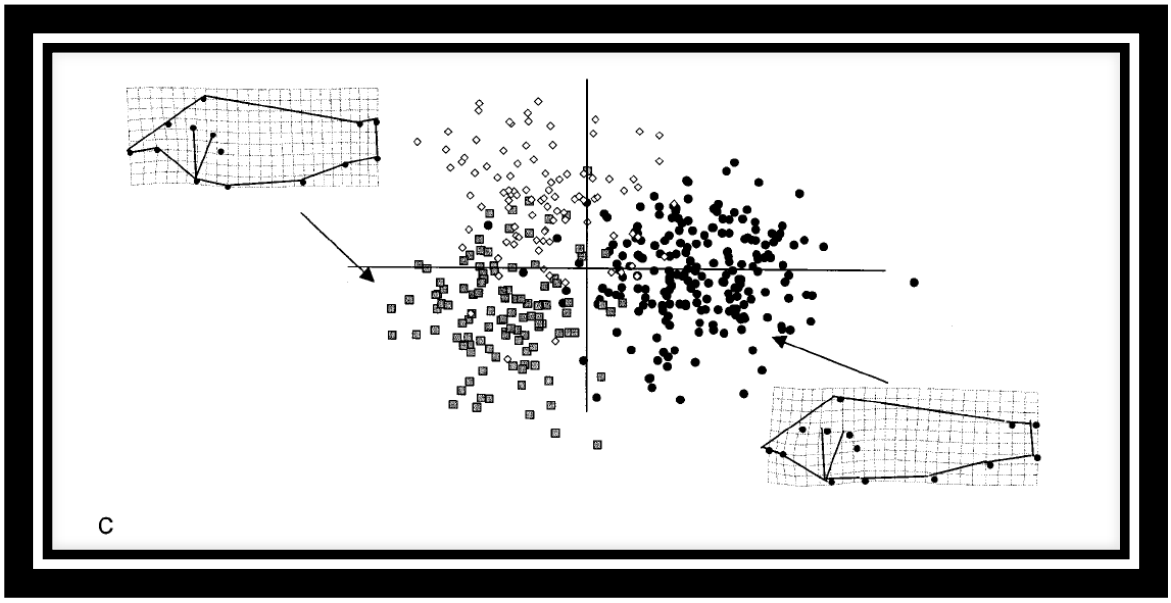

Figure 3: (From Adams et al, 2004) Shape difference visualization via deformation grids

In the early 1990s when geometric morphometrics was recognized as a discipline, it was this ease of visualization that was used as a significant argument for geometric morphometrics to

replace the more traditional morphometrics that employed multivariate analyses of selected distance measurements.[6] Subsequently, the success of morphometrics is largely contributed to the numerous methods of visualization that are able to describe even complex morphological changes far more effectively than the tables of coefficients used in the more traditional morphometric analyses. Most importantly, these methods provide information on morphological differences in their immediate anatomical context, rather than having to be interpreted using the aforementioned tabulated values. Being able to visually recognize and interpret these differences and shape changes remains an important tool for understanding morphological variation.[7] Consequently, geometric morphometrics is being used more and more often to explore answers to an ever growing array of questions in evolutionary biology.[8]

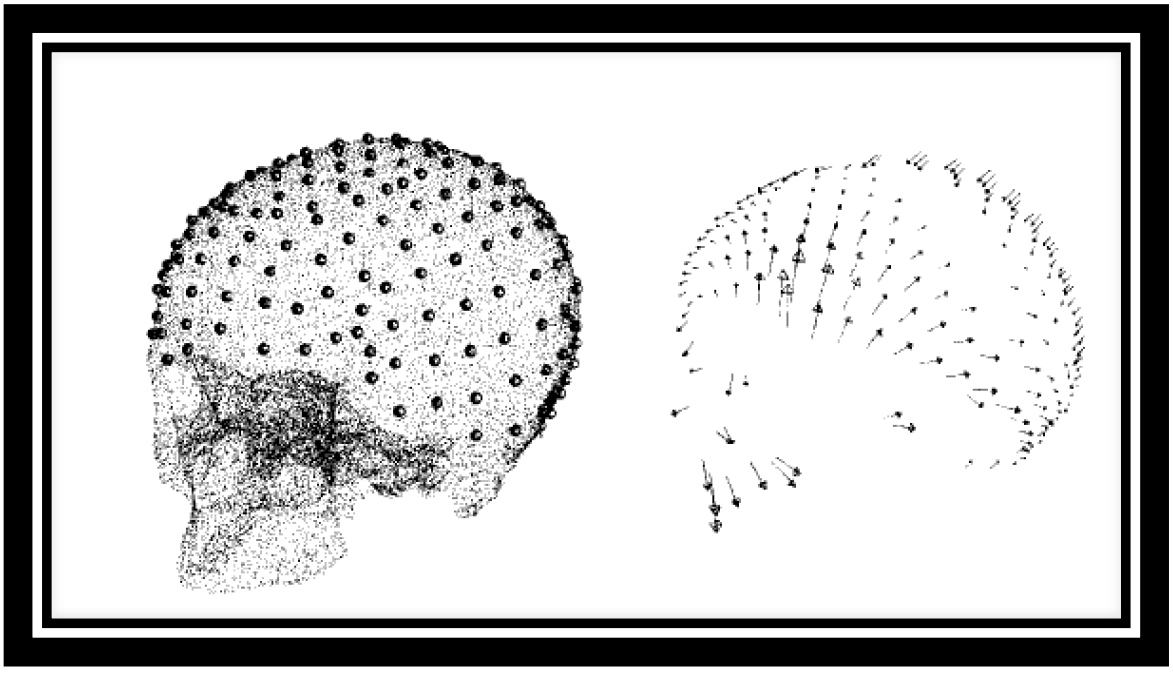

Figure 4: (From Adams et al, 2004) Sliding semilandmarks quantifying the surface of a skull.

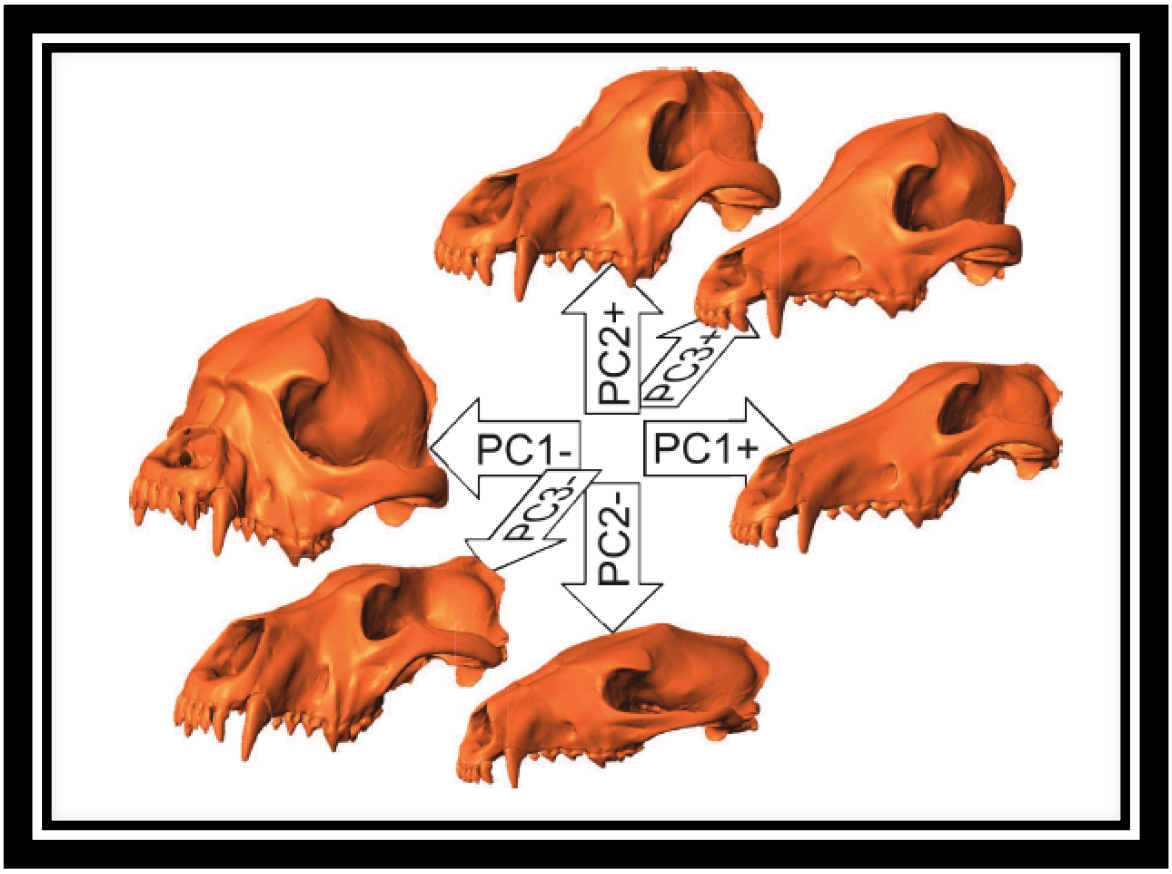

Figure 5: (From Klingenberg, 2013) Warped surfaces according to extremes along principal component axes using thin-plate spline analysis of canine skulls.

C. Mouse Mandible

The mandible has been the focus of numerous anatomical, embryological and developmental analyses by a variety of authors.[9] Consequently, there is a large body of evidence describing its development, morphology and genetics. The mouse mandible itself is comprised of several parts with varying embryological origins and timing of differentiation.[10] Klingenberg et al in 2003 postulated that the mandible also consists of two primary functional units. The first

being the alveolar region, which is located anteriorly and houses the teeth, with the second including the ascending ramus, which articulates with the base of the skull and acts as a point of muscle attachment. Each of these anatomical units, in turn, is made up of several units that are distinctly identifiable and arise from separate cell populations that differentiate at different times[9,10] These include the ramus, the coronoid process, the condyle, the angular process, and two alveolar segments housing the molars and the incisor (Figure 6). These features, along with an extensive foundation of literature, make the mouse mandible uniquely suited as an ideal model system for evaluation of complex morphological traits in conjunction with genomic studies.

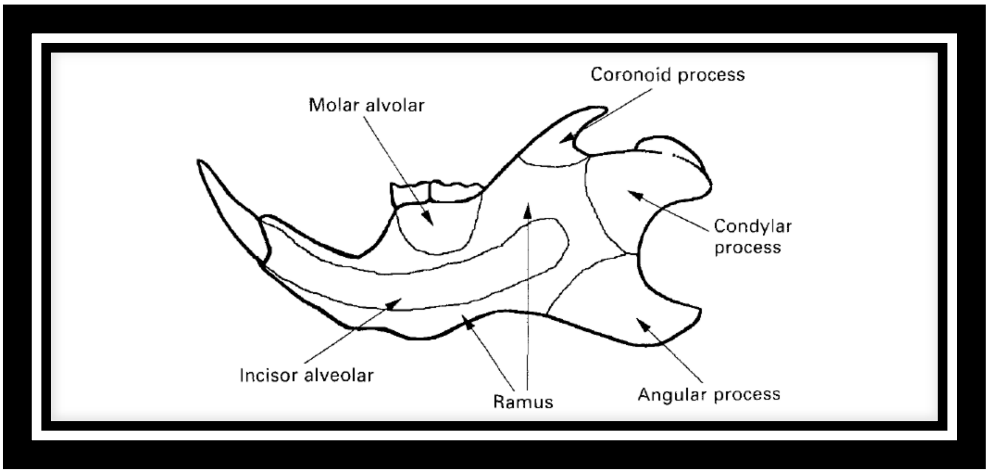

Figure 6: (From Atchley and Hall, 1991) Mouse mandible showing four morphogenetic components (ramus and three processes).

D. Previous Studies

As previously discussed, there has been a steady progression in the field of morphometrics with respect to the sophistication of measurement and analysis. Most of the

advances were made in the last 20 years, and the result has been a multitude of research in the area of geometric morphometrics. Many of these studies have involved evaluation of shape change using landmarks in 2-dimensional space.[10–13]

Klingenberg and colleagues set out to examine the degree of modularity of growth within the mouse mandible. In order to evaluate this they used two-dimensional images of the hemi-mandibles, obtained using a flatbed scanner, and chose 15 landmarks for digitization and subsequent analysis using the Procrustes superimposition method. (Figure 7) They were able to determine that the anterior and posterior portions of the mandible are distinct developmental modules. They also suspected that there may be an additional smaller set of modules in the same areas described in Figure 6, however, they acknowledged that their landmark-based methodology limited the analysis of these areas due to the inadequate number of landmarks contained within these regions.[10]

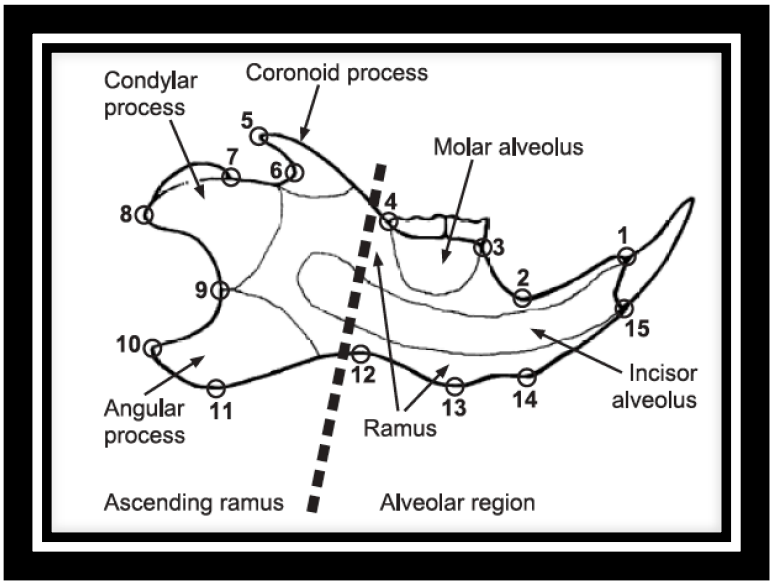

Figure 7: (From Klingenberg et al, 2003) Mouse mandible showing the fifteen landmarks used for Procrustes analysis.

Similarly, Boell and Tautz in 2011 explored the micro-evolutionary divergence patterns of *Mus musculus* populations using a similar method as Klingenberg. Rather than using a flatbed scanner to obtain mandibular images, Boell and Tautz employed a μCT to capture the three dimensional shape of the mandible and then converted the volumes into a two-dimensional radiograph for landmark placement, utilizing 14 rather than 15.[14] (Figure 8)

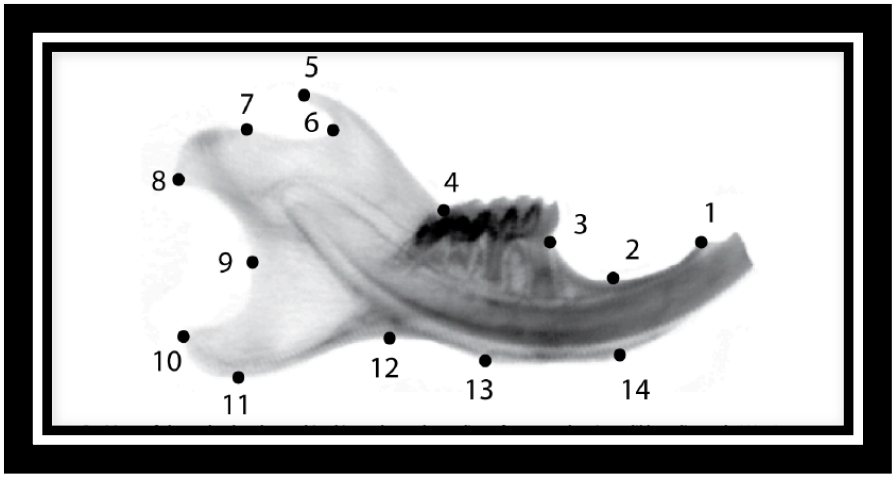

Figure 8: (From Boell et al, 2011) Mouse mandible showing the fifteen landmarks used for Procrustes analysis.

Only in the last five years have we seen some analyses begin to emerge that aim to evaluate shape in three dimensions. Still many other studies continue to use the same, or similar, methodology of capturing a two-dimensional image of the mandible and subsequently placing landmarks.[12,15] Willmore et al in 2009 utilized 2D and 3D methods to compare mouse and baboon mandible phenotypic and genetic integration, finding that the patterns of each is similar between the two.[16] (Figure 9) More recently, Ragheb et al described a method of evaluating shape in three dimensions in order to address what they believed to be some of the shortcoming of current geometric morphometric research.[17] One of the major drawbacks to this approach,

which should be apparent in Figure 10, is the severe burden of landmark placement on the evaluator.

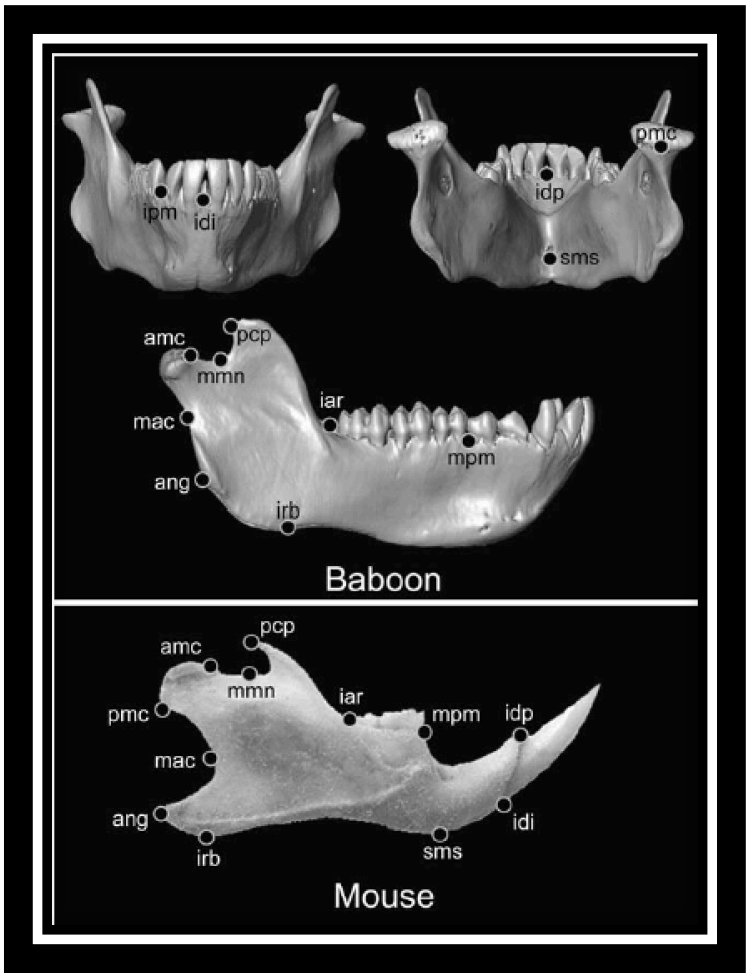

Figure 9: (From Willmore et al, 2009) Baboon and mouse mandible landmark analysis in 3D and 2D, respectively.

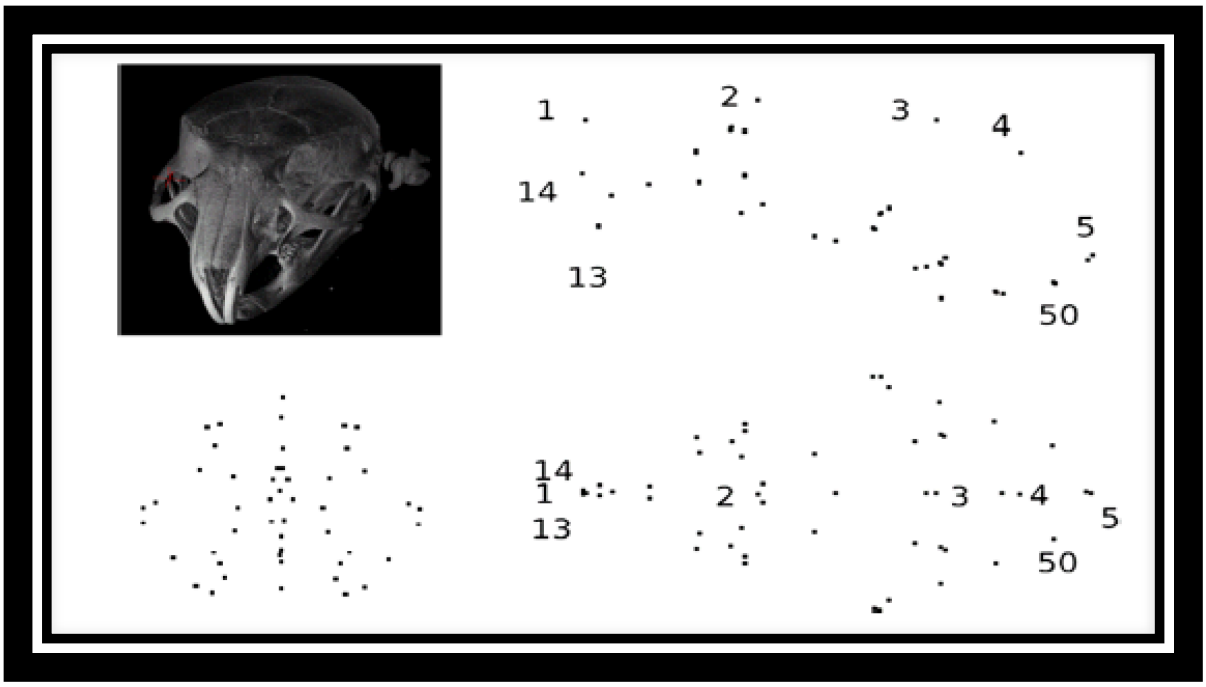

Figure 10: (From Ragheb et al, 2013) Mouse skull showing 50 three-dimensional landmarks used for analysis.

E. Aims of Study

Analysis in two-dimensions and the need for landmark placement are the major drawbacks with the current literature on mandibular shape analysis. This particular study is one component of a much larger ongoing project aimed at characterizing the genetic determinants of mandibular shape using inbred mice in the Hybrid Mouse Diversity Panel (HMDP) from the UCLA School of Medicine. The HMDP is comprised of 29 classical inbred and 71 recombinant inbred mouse strains.[18] The overall project involves three individual but interdependent components: finalizing analysis of mandibular shape in the complete Hybrid Mouse Diversity Panel; generating a gene expression profile of highly heritable and variable areas within the panel; and identification of candidate genes and gene networks for mandibular shape traits. The

immediate goal of the present study relates only to the first component – establishing a novel, landmark-free approach for analysis, comparison, and quantification of morphologic variation and shape changes in the mouse mandible. Once completed, the methods developed in this project should facilitate future endeavors directed at finding areas of maximum shape variance in order to identify candidate genes and gene networks that contribute to mandibular skeletal phenotypes within the HMDP strains. Overall, this portion of the project seeks to explore a way to improve current geometric morphometric techniques used in analysis of mandibular morphology in the mouse by aiming to:

1. Apply a variation on the methodology outlined by Dr. McComb[19] to generate a 3D surface model of the mouse mandible and create an average surface for:
    a) Adult classical inbred strains from the HMDP
    b) Developing mouse at various ages within a single strain
2. Apply and modify the latest technologies used in brain mapping research to identify regional shape differences in 3 dimensions between mandibles free from landmark identification, resulting in identification of heritable quantitative traits.
3. Develop a useful, intuitive and visual method for evaluation of shape differences.

The most immediate application of this methodology will be the ability to visualize specific areas of interest in the mouse mandible much more expediently for further genomic studies; as in the scope of the much larger genome wide analysis study (GWAS) this project is a part of. Should these imaging techniques identify heritable quantitative traits under genetic control, the

possibilities will be endless reaching into numerous fields including orthodontics, evolutionary biology, anthroprometrics, forensics, etc.

Materials and Methods:

In order to accomplish the aims as set forth above, we acquired images using high-resolution 3D μCT, segmented mandibles from the imaged volume and generated mandibular surfaces, and then used landmark-free analytical approaches for geometric morphometric surface mapping of mandibles. Lastly, we used statistical shape analysis to identify interstrain differences within our sample. The general ideas of the methodology within this section are based on and have been adapted from the work of Dr. Ryan McComb.[19] The methodology for this project can be divided into multiple segments, which are summarized below and described in further detail in this section (Figure 11):

A. Collection of intact mouse skulls followed by high resolution μCT scanning
B. Segmentation of sample skull μCT images and surface creation
C. Surface topology correction and surface registration
D. Average creation
E. Shape comparison

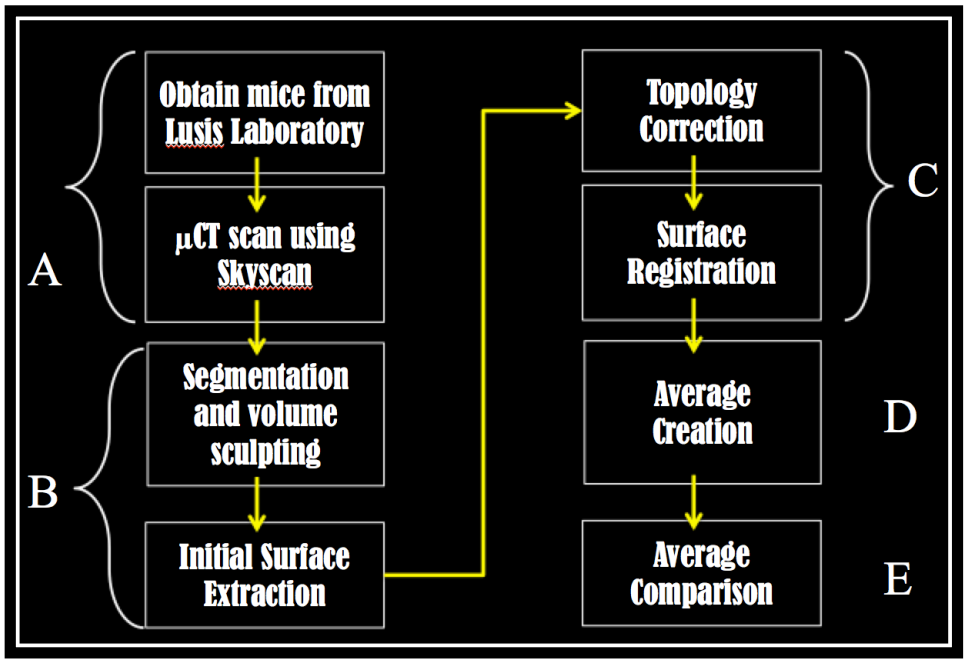

Figure 11: Diagram illustrating the workflow involved in progressing from a single skull to 3D averages and distance maps.

A. Sample Collection

As part of this pilot study, two intact skulls from 4 month-old adult males from each of five parental strains in the HMDP were obtained from the laboratory of Jake Lusis at the UCLA School of Medicine. The strains included C57BL/6, A/J, DBA/2J, BALBCJ, and CH3. (Figure 12) Additionally, because the ultimate goal of the larger study is to identify genes affecting mandibular shape, we felt it was pertinent to determine if we could isolate shape differences in a growing population of a single inbred strain. Accordingly, forty three skulls from a growing longitudinal sample of the strain C57BL/6 were obtained; three at 14 days old, and five at each of the following ages: 21 days, 30 days, 45 days, 60 days, 90 days, 120 days, 180 days and 280 days. (Figure 13) Each of these 53 skulls were then scanned using the SkyScan1172 high-resolution μCT scanner at 55kVP and 167μA resulting in images with 27μm isotropic voxel

resolution. Axial image slices were reconstructed, converted into DICOM format for export into craniofacial analysis software.

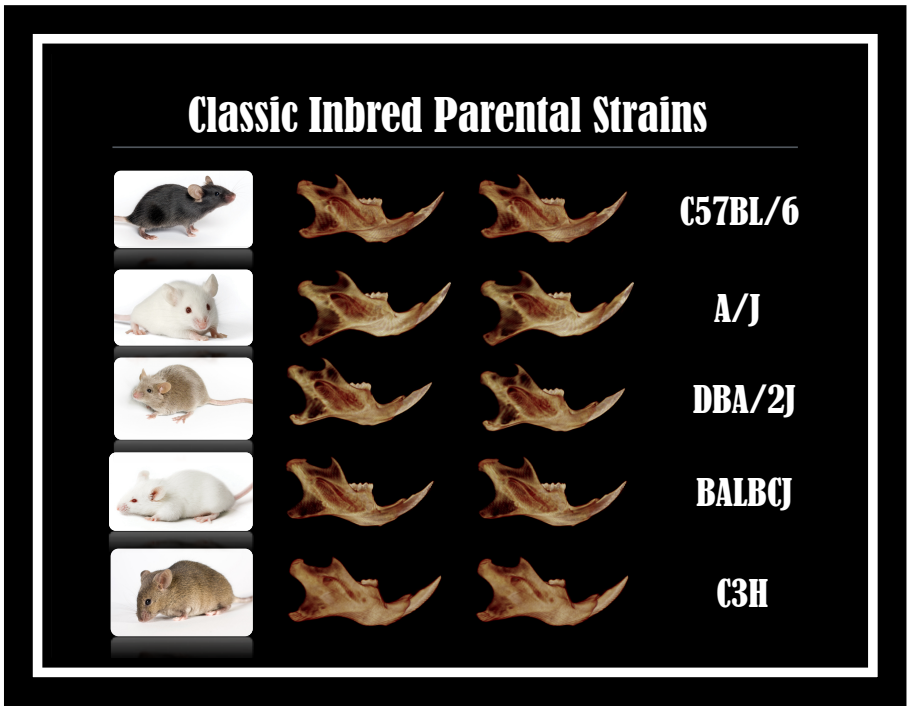

Figure 12: Five classic inbred parental strains from the Hybrid Mouse Diversity Panel

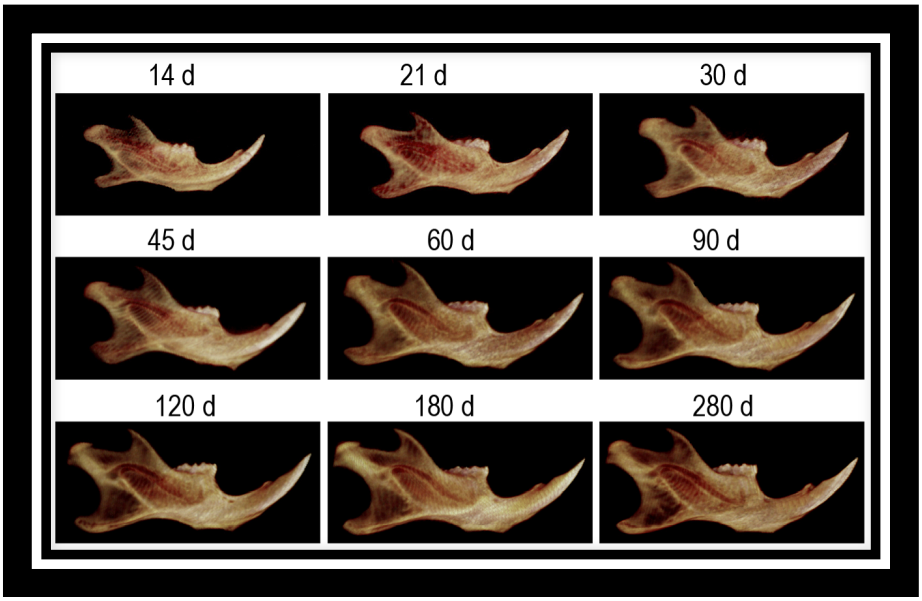

Figure 13: Samples of each age group in the forty-three mouse longitudinal sample of C57BL/6

B. Volume Segmentation/Surface Creation

Images from the Skyscan µCT scanner were then exported in DICOM format into a beta version of Dolphin Imaging® orthodontic analysis software, version 11.7, that was capable of handling the high resolution of the µCT scans. Hemi-mandibles were then segmented from the entire skull volume using the volume-clipping tool. (Figure 14)

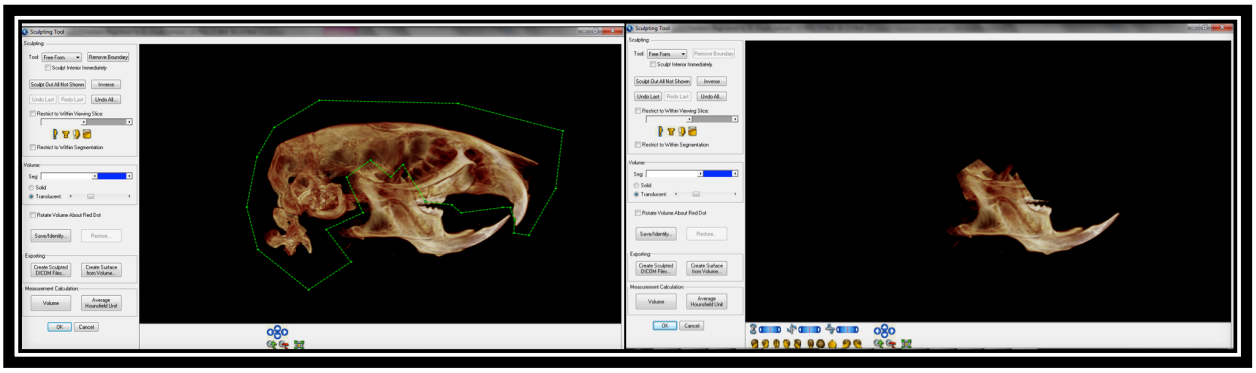

Figure 14: Segmentation of mandible from complete skull using Dolphin Imaging® 11.7.

After the mandibles were segmented, they were opened in the surface extraction module of Dolphin and adjusted for optimum hard tissue resolution using a sliding scale to minimize both noise and pseudofenestrations as described by Schunke et al in 2012.[20] (Figure 15) Sixty-three hemi-mandibles in all were included in the study (20 from the five parental strains, 10 right and 10 left; 43 right hemi-mandibles from the longitudinal sample). Once segmented and the threshold adjusted, three dimensional surfaces of each mandible were created by generation of

nodes on the surface of each image to fabricate a triangular mesh of approximately 150,000 vertices (per hemi-mandible) for subsequent processing. (Figure 16) Because we sought to evaluate hemispheric differences within our sample as well as increase sample size for increased significance, the surfaces created for the 10 left hemi-mandibles were mirrored using the high end 3-D animation software Houdini (Side Effects Software, Toronto), to create and additional 10 right hemi-mandibles as previously described.[21,22] This resulted in 20 right hemi-mandibular surfaces for analysis. For the longitudinal sample consisting only of the C57BL/6 strain, just the 43 right hemi-mandibles were used for analysis.

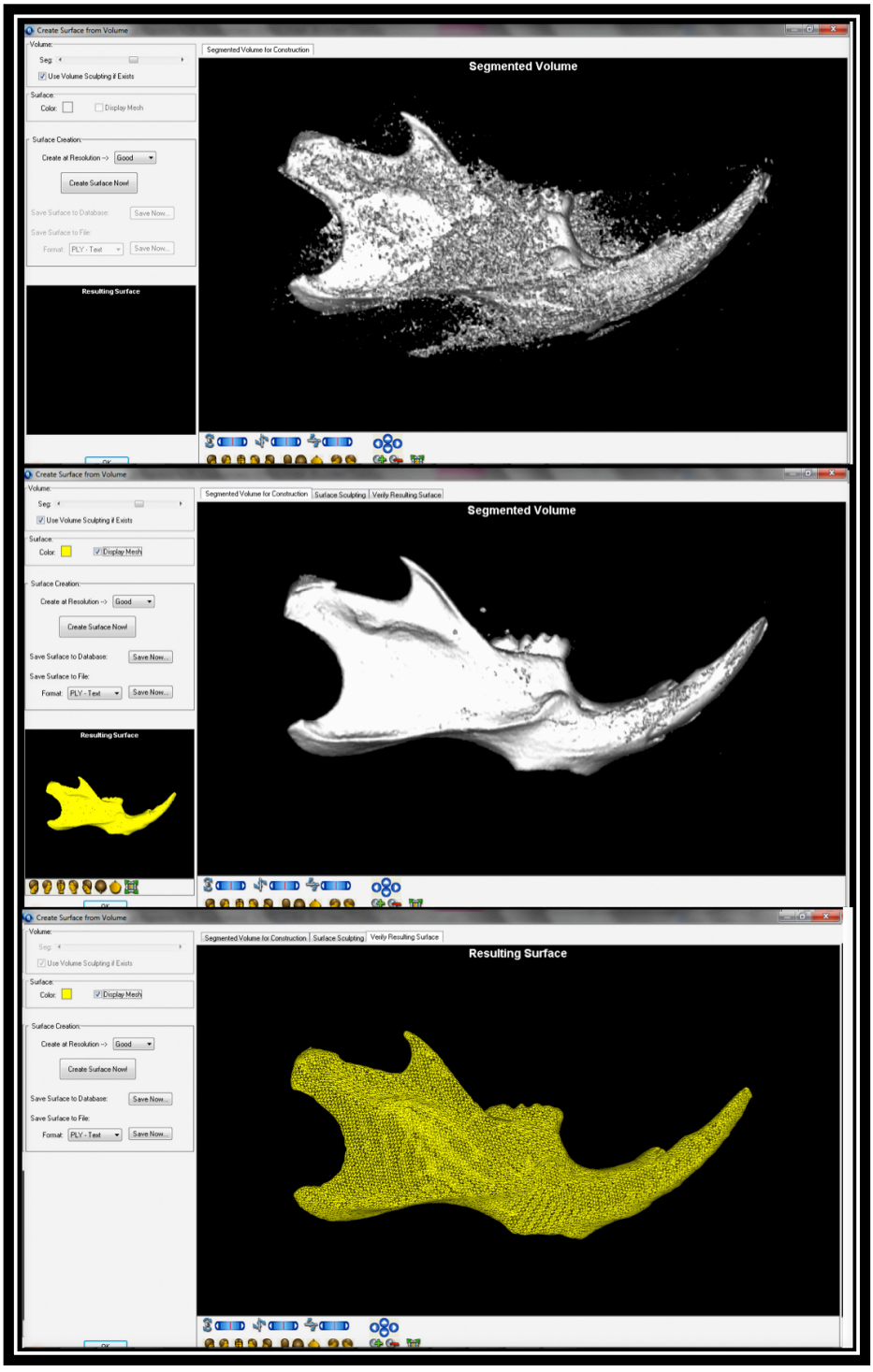

Figure 15: Threshold determination and surface creation of hemi-mandible using Dolphin Imaging® 11.7.

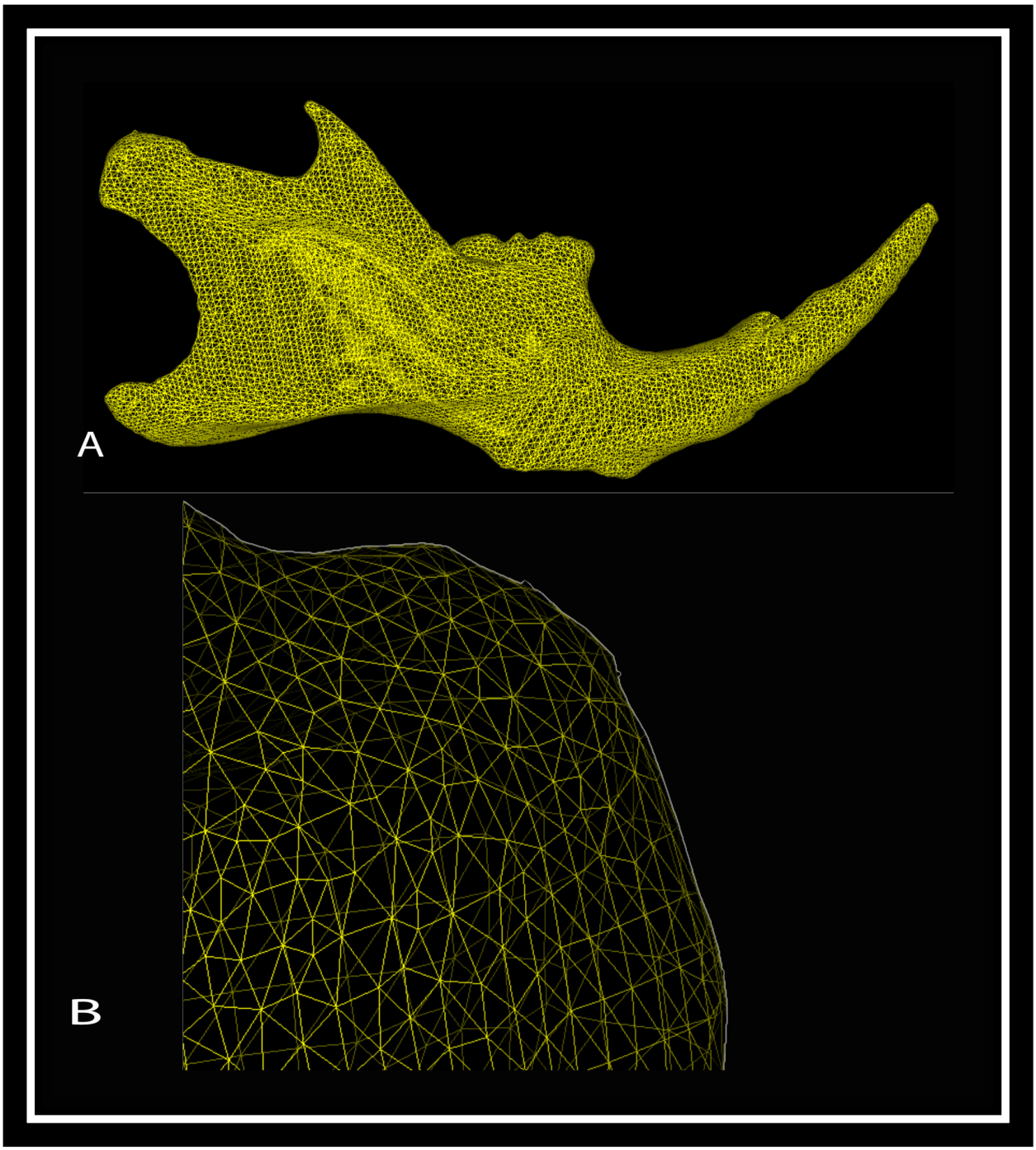

Figure 16: A) Surface mesh of hemi-mandible. B) Magnification of the molar area to illustrate the intricate mesh framework of 150,000 vertices created using Dolphin Imaging®.

Once the surfaces were refined and meshes created, they were exported and saved in a binary text .PLY format (Polygon File Format). This format is used to store 3-dimensional graphical data of objects described by a series of nominally flat polygons.

C. Topological Correction of Surfaces (*in collaboration with B. Gutman, LONI)*

Modification of surface topology is needed when the generation of certain artifacts such as unnecessary handles results from surface creation.[23] In order to compare mandibular surfaces with varying topology, careful coordination of the samples must be established, but this cannot be done without topological correction. This was not without similar challenges as described by McComb in 2012. Additionally, noise is a very important consideration when evaluating CT images. In general, the lower the signal-to noise ratio the lower the CT image quality.[24] Yet despite the high resolution of the μCT, there was still significant noise surrounding parts of the samples. Excess noise results in the creation of surfaces with highly variable topology, which must be altered before correspondence can take place. Following the methods as described by Han et al in 2003, we were able to correct the topology of the mandibular meshes to eliminate both handles and boundaries.[25,26] As the resulting mandible models had spherical topology, the natural parameter space to perform a correspondence search for all subjects' meshes was the 2-sphere. To do this, the mandibular shapes were first mapped to a sphere following LONI's application of unconstrained spherical parameterization as set forth by Friedel et al in 2003, one of the top state-of the-art spherical mapping tools currently available.[27] (Figure 17)

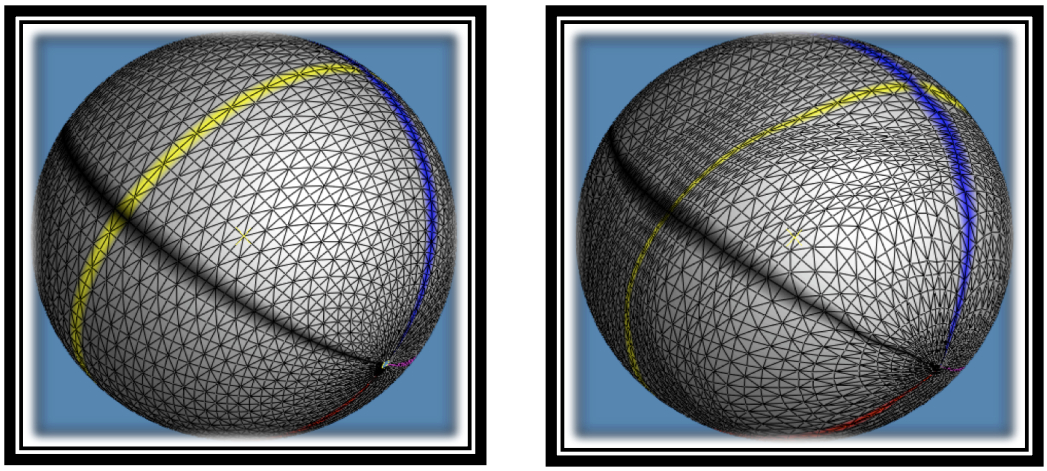

Figure 17: (From McComb 2012) Spherical representation of a surface mesh in original and warped form.

D. Shape Registration and average creation (*in collaboration with B. Gutman, LONI)*

Borrowing methods from the fields of neuroimaging and brain mapping,[28–32] we were able to compare the various mandibular samples through parametric registration and resampling of the surfaces to the same number of mesh points, with exact point-to-point correspondences across all subjects. However, due to the fine resolution of the μCT scans, surface meshes generated in Dolphin produced more vertices than necessary (150,000) to represent the anatomy of the hemi-mandibles. In preliminary tests, we found that reducing the number the nodes on the mandibular surfaces to a more manageable working resolution of 7500 vertices was more than adequate to accurately capture the details of mandibular shape.

A representative model was chosen as the initial target for registration. Point-to-point correspondence was achieved between meshes of this reference shape and all samples by flowing the vertices of each hemi-mandible on a spherical domain in order to minimize geometric

distortion and differences in the mean and Gaussian curvatures of the shapes at each point. (Figure 18) Because these elements are principal shape characteristics, final shape correspondence was reliable and anatomically accurate. To ensure smooth invertible spherical warps, we used the viscous fluid framework adapted to the sphere. The fluid approach has been shown to be useful in image correspondence,[33] with multiple studies implementing it over the years.[34,35] A more recent variation of this method by Shi et al,[36] registers shapes to a flat two-dimensional domain. While decent registration results for brain shapes similar to mouse mandibles were achieved in this study, it required manual definition of boundaries on each shape so they would correspond to boundaries of the rectangular parameter domain. To permit a more fully automated registration of shapes for this project, we used the fluid framework model directly on the sphere, as described by Gutman et al.[37] Using this methodology, no landmark identification is required moving us closer to a more automated solution.

After parametric registration of the shapes, the population average surface was computed for the hemi-mandibles of all five strains. (Figure 19)

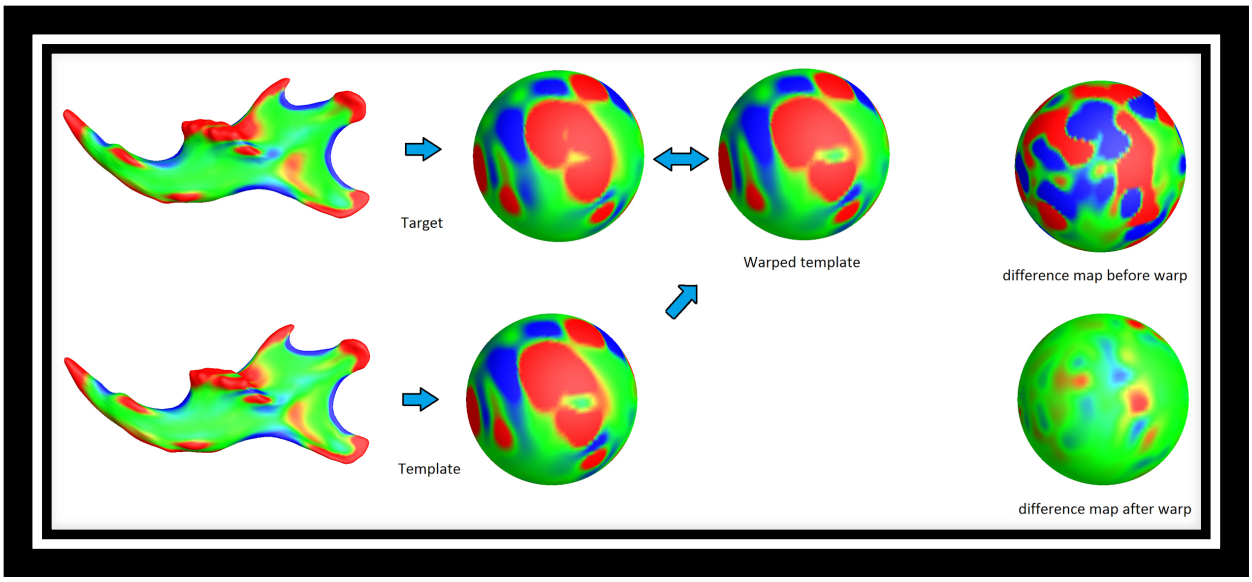

Figure 18: Sample Gaussian curvature maps, matched on a sphere

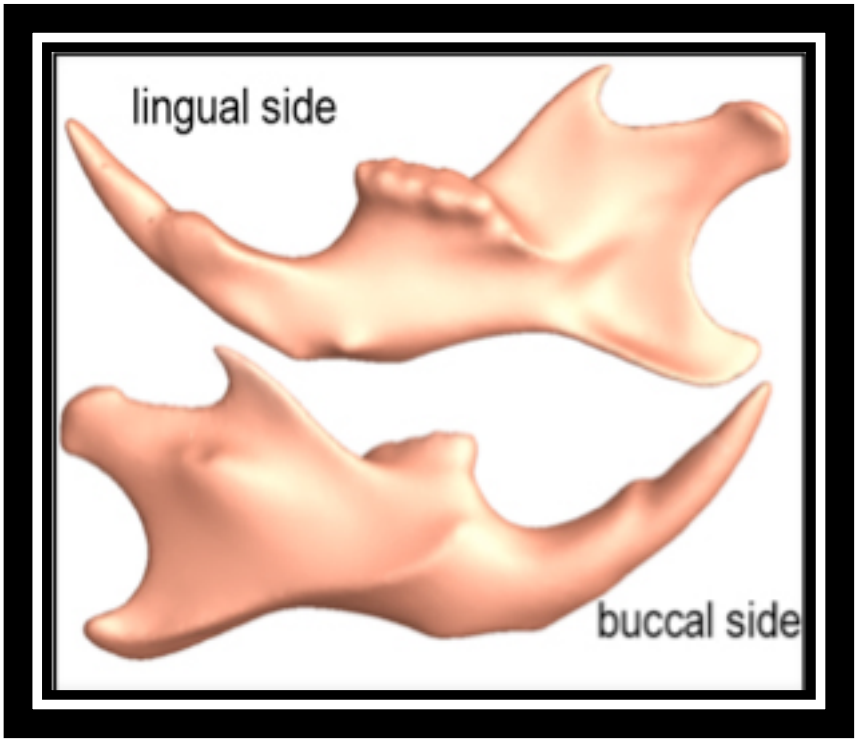

Figure 19: Average mandibular surface created from five strain population

E. Shape Comparison

Initially, we explored several methods for shape comparison including medial axis,[38] curvature-based evaluation centered on principal curvatures[39–41], and tensor-based morphometry.

a. Medial Axis

With the first approach, we used mathematical algorithms to compute the 1D medial axis of the mandible, and compute the thickness of the bone as distance from each mesh point to the axis. (Figure 20) Statistical analysis is then performed at each homologous point. (Figure 21) Because each point was assigned a significance value, we were able to place all p-values directly onto the shape, creating a visually beneficial color map, or "p-map". (Figure 22) Creation of "p-maps" permits us to facilitate interpretation by allowing a clearer visualization of shape difference.

Aditionally, in an effort to validate the method, we took a single strain (C57BL6) and compared the right and left mandibles to each other using the medial axis. We also randomly chose strains C57BL6 and AJ and compared them to each other.

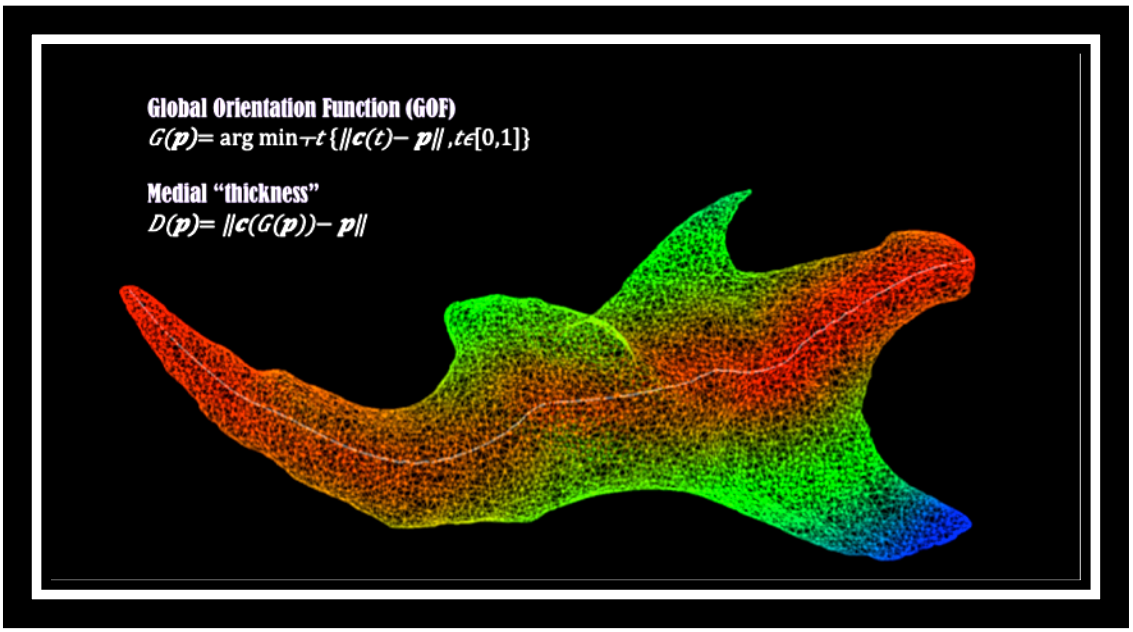

Figure 20: Construction of medial axis.

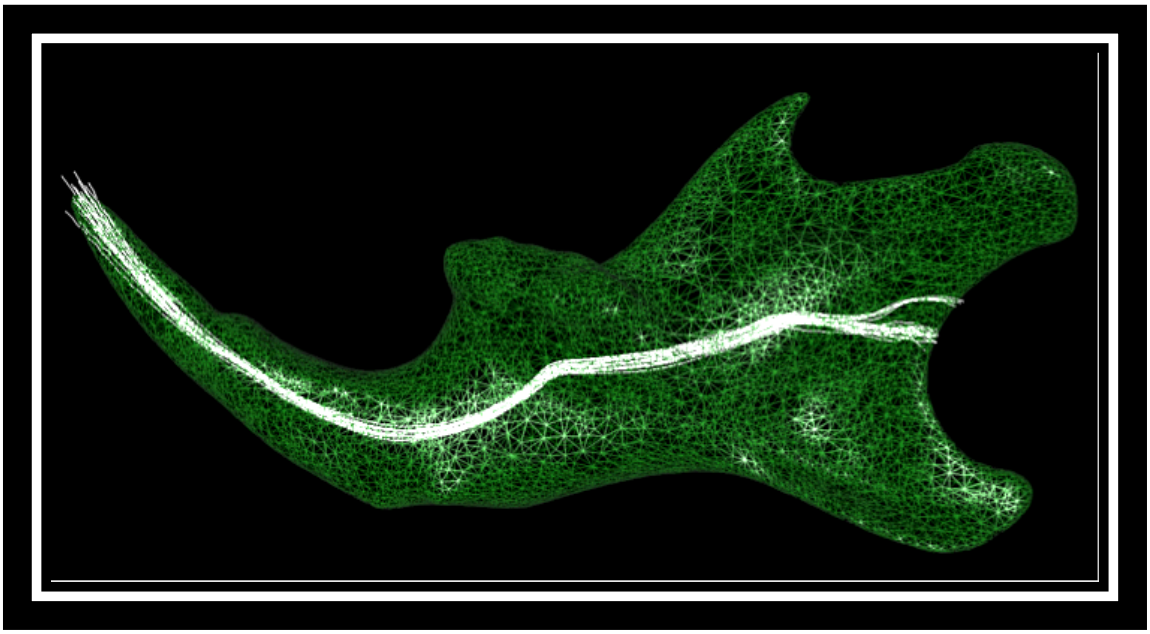

Figure 21: Alignment of samples along medial axis for shape difference evaluation.

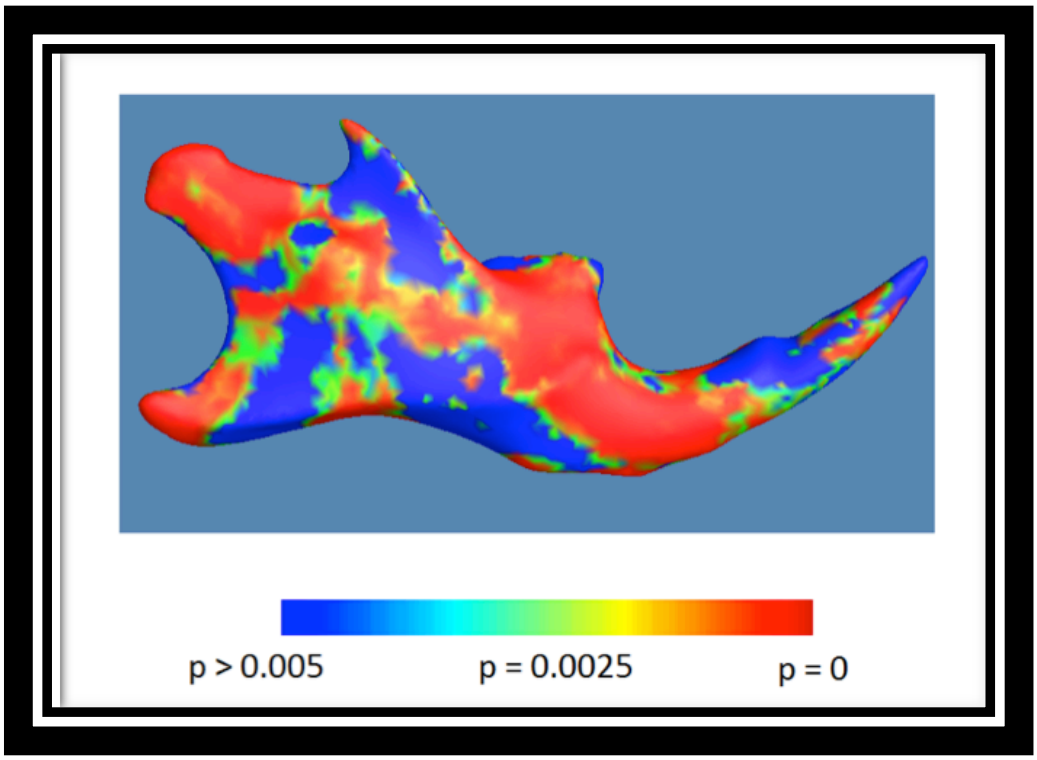

Figure 22: Example of a "p-map" displaying statistically significant areas of shape difference.

b. Principal Curvature-based Measurements

Next we explored a curvature-based measurement technique, commonly utilized at the Laboratory of Neuroimaging that measures and compares the intrisic curvature of two surfaces. By comparing the principal curvatures (**K1** and **K2**), or the maximum and minimum of the normal curvature, at each point, we are able to measure how "sharp" an edge or cavity is, or how "sphere-like" a local patch is. It's good for complicated structures with large variation from one to another and a similar general curvature skeleton. It does not, however, produce a very stable measure. We applied this methodology it in the mandible (Figure 23), but it was too noisy and unstable, requiring smoothing. Unfortunately, smoothing in this application results in partial volume effects. As a result, the outcome was not as intuitive and deemed unsatisfactory.

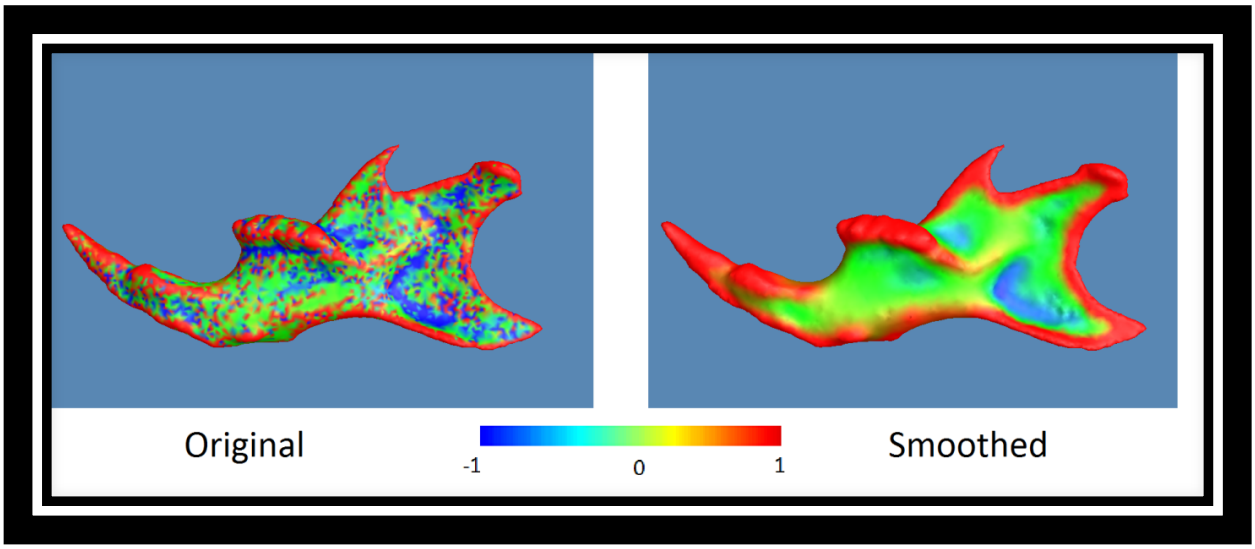

Figure 23: Curvature based evaluation using principal curvatures k1 & k2, showing both the original and smoothed maps.

c. Tensor-Based Morphometric Analysis

Dr. Paul Thompson's team at the Laboratory of Neuroimaging (LONI) has successfully adapted morphometric techniques and shape analysis tools to evaluate other areas of the human body, and has published work outside of their current discipline of brain imaging. For example, they have written tensor-based morphometric (TBM) tools to evaluate the three-dimensional shape of femoral cartilage in osteoarthritis patients,[42] the genetic component of shape variation within the human face,[43] and a series of articles demonstrating techniques for facial recognition utilizing three-dimensional surface meshes.[44,45]

Having already achieved high-quality point-to-point surface correspondence, we then calculated measures of the various shapes to be compared directly across surfaces at every

homologous point. Using these points and following Wang et al 2011, we applied the surface Tensor-based Morphometry (TBM) to each of the mandibular shapes. TBM is a geometric morphometric methodology that analyzes the Jacobian tensor of the deformation between a pair of images[46,47] or surfaces.[30,36,48] This method allows us to examine several complimentary measures, which considers overall dilation, directional stretching or the full Jacobian tensor at every corresponding point.

Our final reference shape was the population average surface (Figure 19). In order to make the final correspondence unbiased, we used the average shape template computed from the individual target-based registration to recalculate the correspondence for all shapes. This ensured that the final correspondence and the resultant TBM measures were more robust. As mentioned previously, to compare mandibular shape across hemispheres, we reflected all left hemi-mandibles and mapped shapes into one coordinate system.

To evaluate the Jacobian determinant across strains at homologous points, we used a standard mass-univariate test. More specifically, in order to assess the Jacobian variation for both hemisphere and strain, we employed a 2-way ANOVA. This resulted in an F-score and p-value for each point in three categories: (1) hemispheric difference, i.e. significant asymmetry in all strains, (2) strain difference, i.e. significant variation in both hemispheres according to strain, and (3) strain-hemisphere interaction, or any difference in asymmetry based on strain. The ultimate goal of performing this mass-univariate analysis is for the visualization of regions that significantly vary between strains. "P-maps" were also created as described above.

Consistent with proven statistical comparisons for shape analysis,[15] we also decided to apply Principal Components Analysis (PCA) to our shape measures in order to identify principal components (PC's) that best illustrate interstrain variation. Traditionally, PCA is used with Procrustes coordinates formatted in two or three-dimensional space, based on sample and landmark choice, thus the feature space is designated as such. However, the feature space we used for our analysis includes the tensor-based morphometric measures at each mesh point. Despite being much bigger than the traditional method, the feature space we employ is composed entirely of intrinsic components of the particular shape, and not created by the indiscriminate nature of Euclidean coordinates based solely on association between neighboring landmarks.[7] We also performed 2-way ANOVA on each component, similar to the previous step. To visualize PC's in this feature space, we created heat maps indicative of relative strength and direction of variation at each mandibular location for each PC. Thus, areas marked with cool colors contract as one moves along the principal direction, while those marked with warm colors expand. The ANOVA aims to localize quantitative traits for heritability analysis, while the heat map creates of intuitive, visual reference figures. (Figure 24)

The same protocol was performed on the longitudinal sample of 43 mice at successive ages within the C57BL/6 strain and color maps were generated.

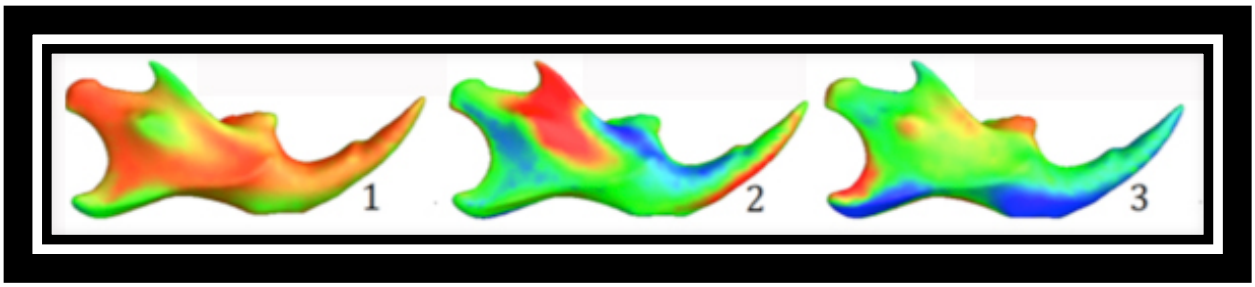

Figure 24: Principal component analysis heat map example

d. Landmark-based Procrustes Superimposition

We also wanted to explore how our results with TBM would compete with those calculated using the widely accepted landmark-based Procrustes superimposition method.[16,49–52] To accomplish this, we placed 22 landmarks in three-dimensions on each of the parental strain segmented mandibles (using the same Dolphin Imaging® software as above) and performed Procrustes alignment using the MorphoJ software as described by Klingenberg[53] (Figure 25) Following Procrustes superimposition, principal component analysis was performed on the three-dimensional coordinate system of landmarks and the heritability of the PC's was analyzed.

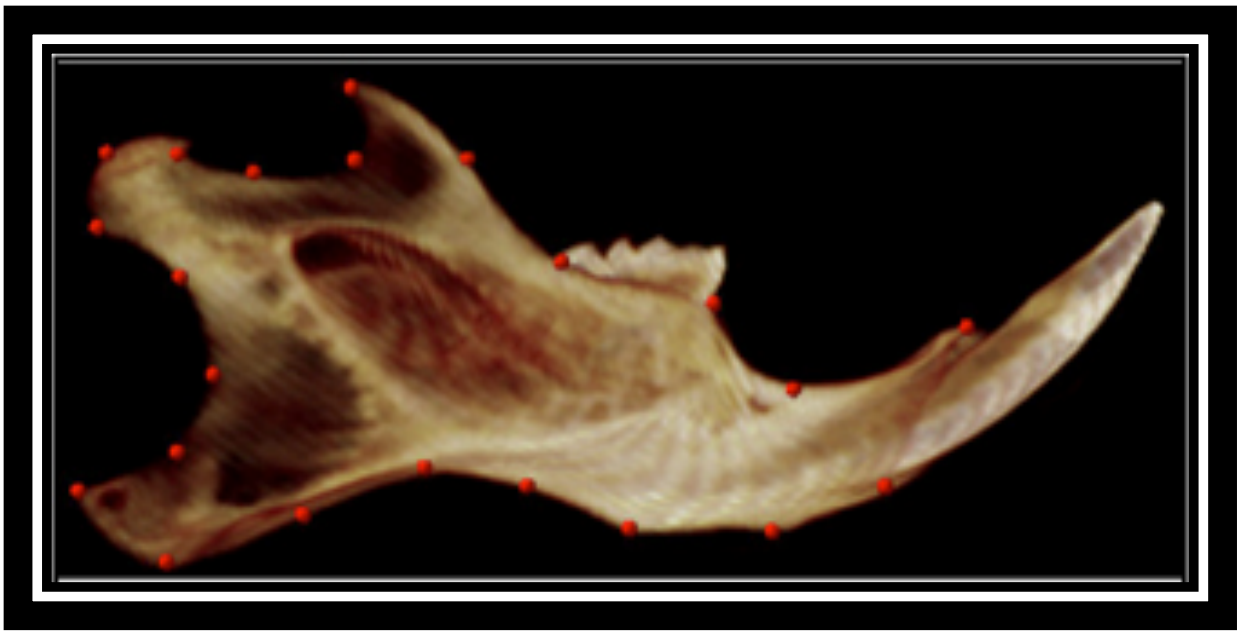

Figure 25: 2D rendition of 3D Procrustes landmarks for superimposition.

Collaboration with B. Gutman at LONI resulted in the development of a similar, albeit simpler, 'pipeline' as contained in the protocol set forth by McComb.[19] (Figure 26)

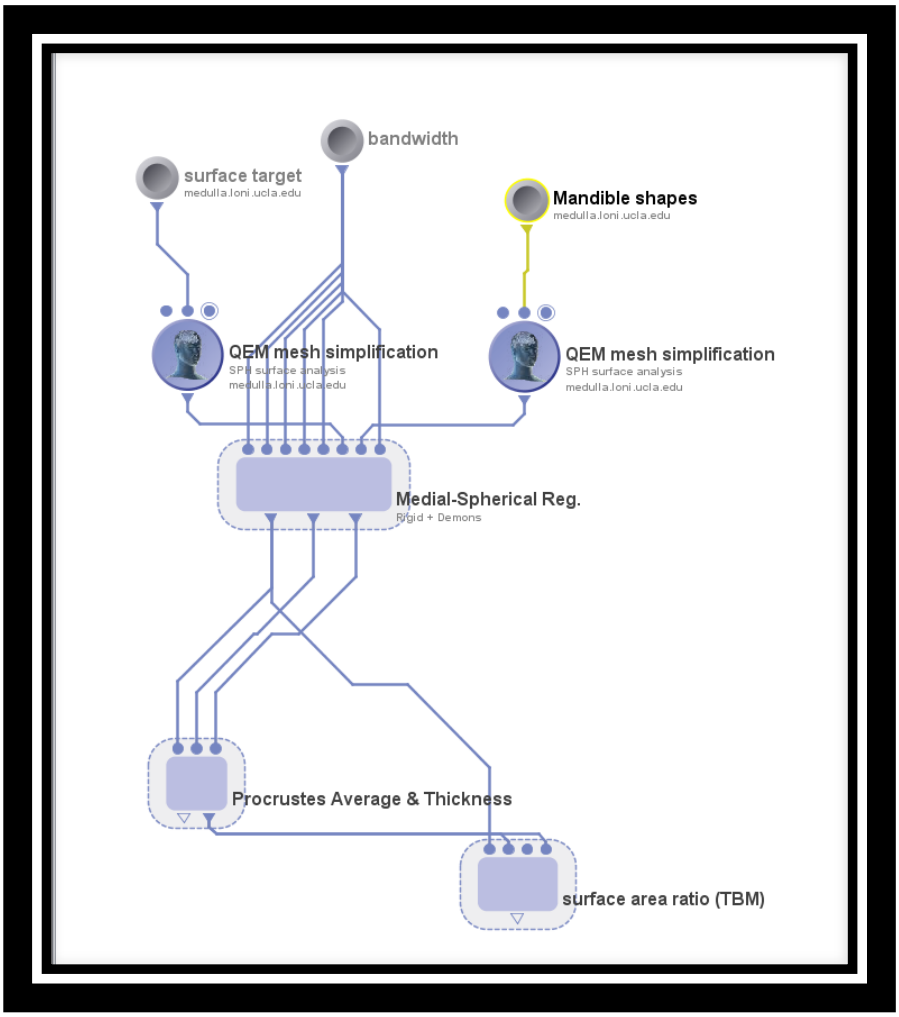

Figure 26: Snapshot of LONI pipeline used to analyze mandibular shapes.

Results:

Curvature-based analysis yielded results that were too noisy and too difficult to localize. (Figure 23) Consequently, there was little in the way of useful and interpretable data and was thus discarded from the study. The medial axis methodology, however, did prove useful in

identifying areas of shape variation. As we can see from the color map (Figure 27), there are a number of areas of statistically significant shape difference between strains.

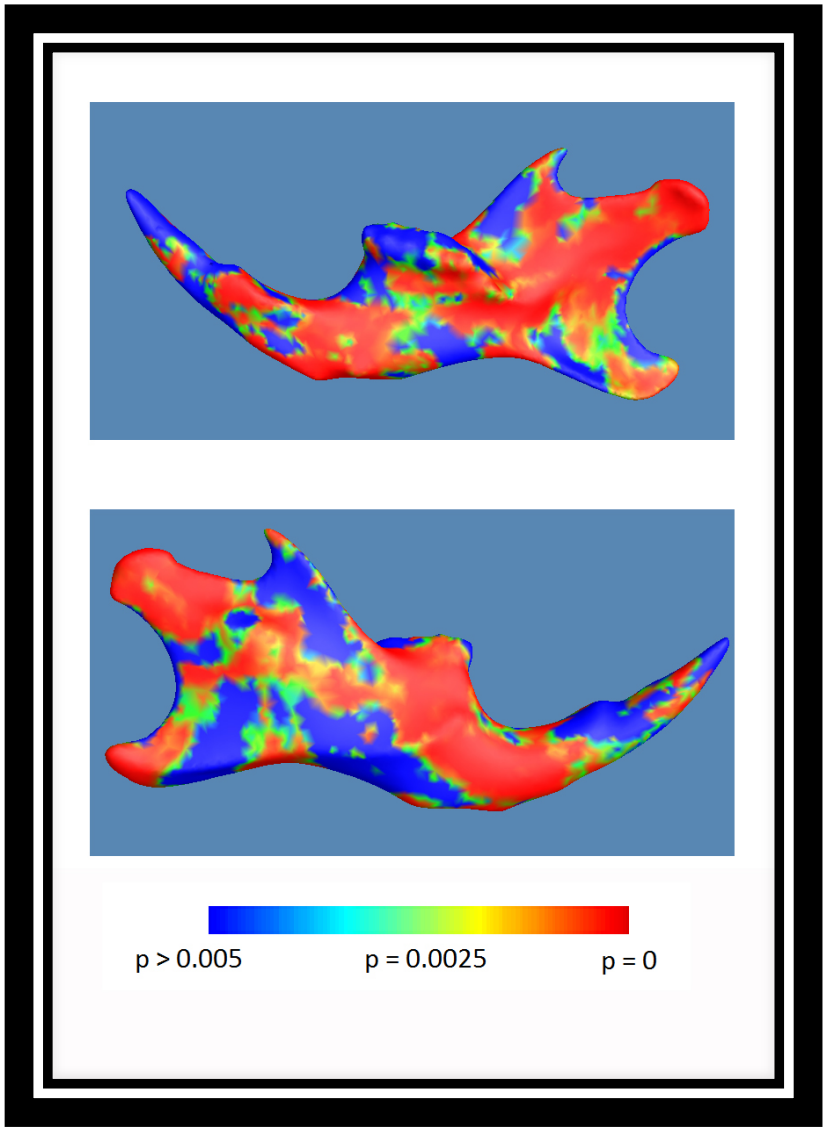

Figure 27: Areas of statistically significant interstrain shape variation developed using the Medial Axis methodology.

For further confirmation, the medial axis technique was applied to animals within the same strain, as well as two randomly chosen strains. As we expected, there was no statistically

significant difference between the shapes of the intrastrain mandibles as indicated by the color map. (Figure 28) For the two random interstain samples we obtained similar, though understandably different, results than for the full interstrain sample. (Figure 28)

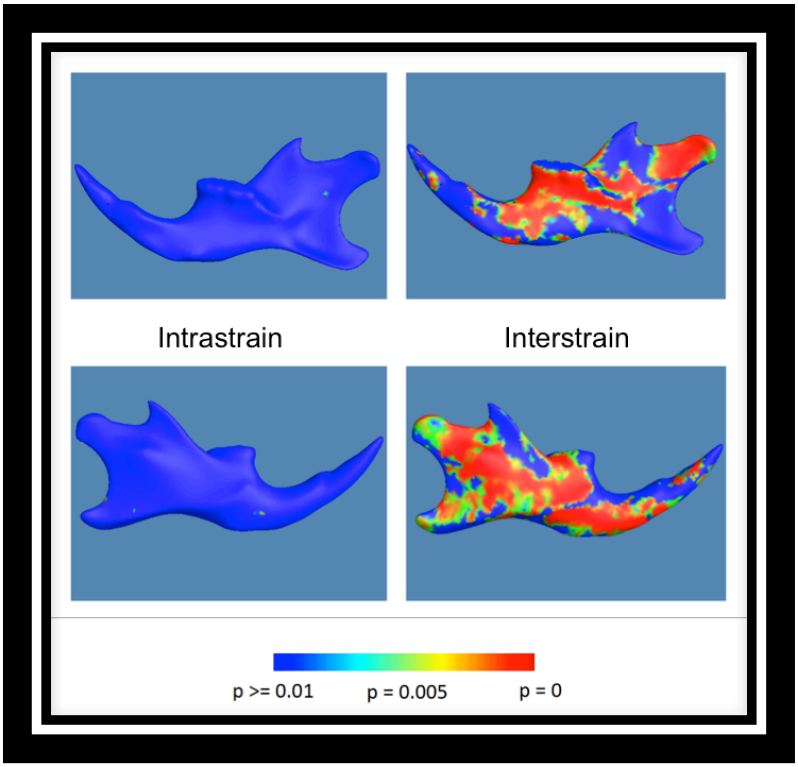

Figure 28: Medial axis interstrain and intrastrain variability validation.

Results of tensor-based morphometrics coupled with ANOVA were similar to those found using the medial axis, though more specific. (Figure 29) Additional findings showed extremely low intrastrain variability compared to the interstrain variability of shape differences when using TBM. Due to the enormous number of mesh points used in TBM, we applied a False Discovery Rate (FDR) correction as described by Langers et al to the mass-univariate F-test, which passed with q = 0.0377. [54] The largest F statistic of a PCA-based F-test was 69.8 with a p-

value of 2.89×10^{-7}. This is critical because it allows us to conclude that phenotypic traits are discernable across the five strains using this method.

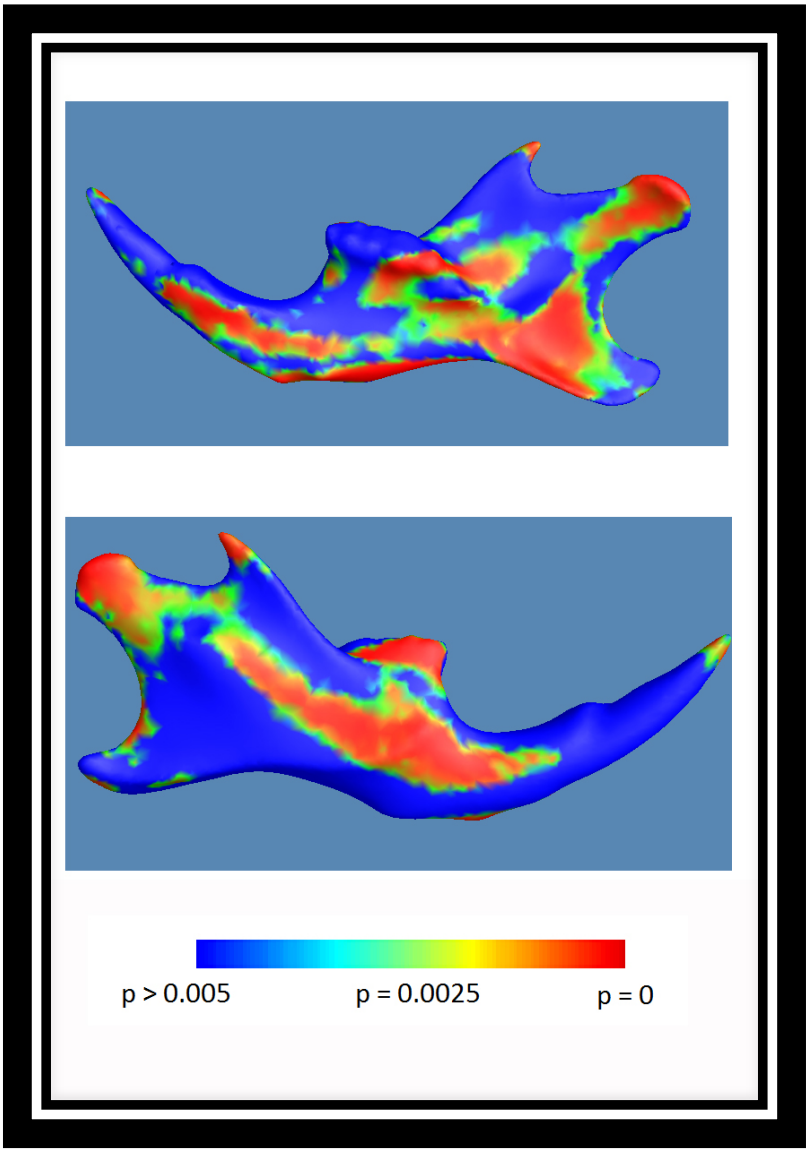

Figure 29: Areas of statistically significant interstrain shape variation developed using ANOVA and Tensor-based Morphometric techniques.

Through the application of PCA-based ANOVA coupled with tensor based morphometric analysis, we were able to identify four significant components of interest with respect to shape variation within our interstrain sample. (Figure 30) Significance values for the first four principal components are also given here. These color maps are representative of the principal components and characterize the directions of maximum variability within the high-dimensional feature space. Alternatively, shrinkage displayed by areas in blue is associated with expansion in the red areas for a given component. Some of these principal components were plotted by strain to illustrate the high heritability of these traits. (Figure 31) We note that in this figure, for example, with respect to PC2, C57BL6 and BALBC have the greatest variation for this trait. Similarly, AJ and DBA show the greatest variation for the trait described by PC3.

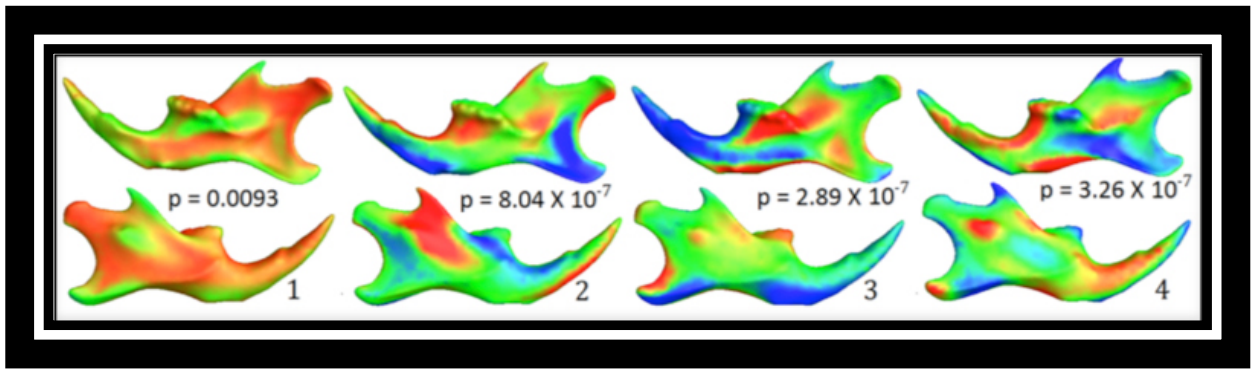

Figure 30: Visualization of prinicipal components created using tensor-based morphometry. Numbers nestled between hemimandibles show the F-test (ANOVA) significance for heritability

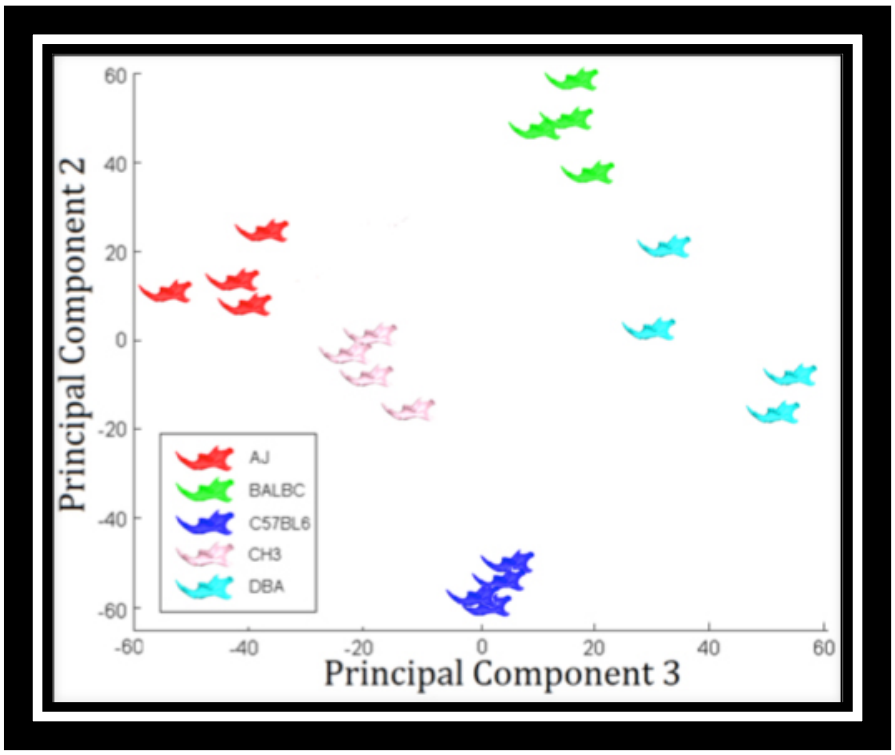

Figure 31: Scatter plot of PC2 vs PC3 for principal component analysis by strain.

None of the components were identified as significant for interaction or hemispheric differences. We did note that the first principal component did not survive Bonferroni correction. Heritability test results confirmed that the 4 PCs were significantly indicative. All of the strains showed at least 95% heritability for a minimum of one trait with he highest heritability reaching 99%. Additionally, the first four PC's explained 79% of the total variance.

Results using MorphoJ for the landmark-based Procrustes method on the interstrain sample were similar to, though slightly inferior to those obtained by TBM. The highest heritability by strain had a range from 89-99% and the first four principal components explained only 67% of the total variance.

The aforementioned results refer to shape differences found in four month old male mice, an age at which mandibular growth is complete and its final shape has been determined. However, as part of a larger study designed to discover the genetic determinants of mandibular shape, we thought it pertinent to apply TBM to a sample through various stages of mandibular growth. TBM and statistical analysis was performed similar to the interstrain sample and the results were charted on a color map. (Figure 32) For ease of visualization, the scale difference was adjusted for the stage between 14-21 days where the most significant shape change is seen.

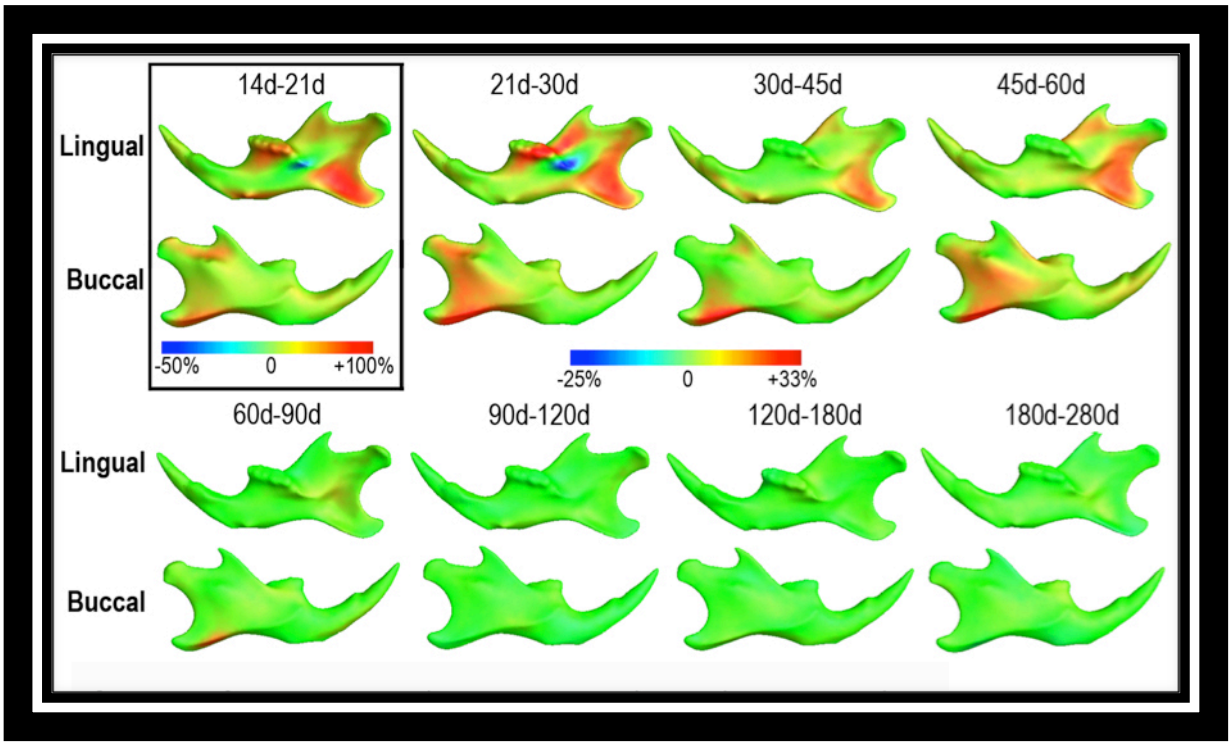

Figure 32: Color maps for intrastrain (longitudinal) sample showing areas of localized shape change using TBM

If we look to compare the results from these two methodologies, it is easy to visualize areas in which they agree significant variation in mandibular shape exists. (Figure 33A,B) Interestingly, results from the 14-21 day age group, with the most drastic shape change within the longitudinal sample, displayed similar finding to both the medial axis and TBM results for interstrain variation. (Figure 33C) Consequently, we were able to identify four distinct areas of interest, including the condylar process, angular process, inferior border and alveolar ridge.

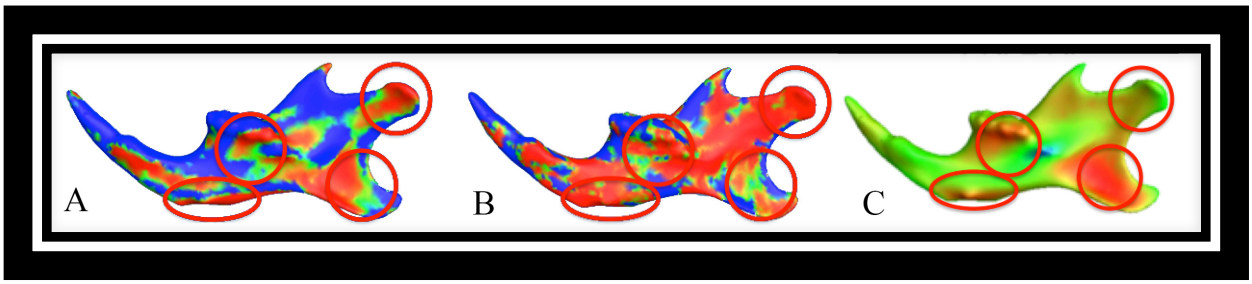

Figure 33: Comparison of results confirming distinct regions of interest for A) TBM (interstrain), B) Medial Axis (interstrain), and C) TBM (longitudinal).

Discussion:

This study was directed at exploring innovative and efficient methods for evaluating shape variation in the mouse mandible while preserving efficacy. As mentioned previously, the specific aims of this study were to:

1. Generate a 3D surface image of the mouse mandible and create an average surface for a cross sectional sample of parental strains in the HMDP, as well as a developing longitudinal sample within a single strain.
4. Apply and modify the latest technologies used in brain mapping research to identify regional shape differences between the mandibles of these samples in 3 dimensions

without the use of landmark identification, with the ultimate goal of identifying heritable quantitative traits.

5. Develop a useful, intuitive and visual method for evaluation of shape differences.

We were able to address Aim 1 and create average mandibular shapes for the populations using the methodology described by McComb.[19] (Figure 19) Additionally, with reference to Aim 2, we successfully applied independently validated techniques used in the field of neuroscience to identify areas of significant shape variation in both the interstrain adult and developing intrastrain mandibular samples. These areas also passed heritability tests suggesting that the development of these areas is under some degree of genetic control. Lastly, according to Aim 3, we were able to produce visually pleasing, easy to follow color maps for each sample.

Our results using the interstrain sample suggest that traditional landmark-based analysis is inferior and less reliable with respect to the ease of visualization and co-localization of shape variation when compared to TBM. We also show TBM offers slightly greater specificity for heritability (95-99% vs. 89-99%) and explained more of the variance (79% vs. 67%). A possible reason for this may be that TBM considers local area dilation while landmark-based procedures do not. The effect is that TBM is truly a 'local' method. In other words, whenever there is a difference in the dilation factor at a distinct point on the surface and it is determined to be significant between strains, one can be assured that it is at this location that the two shapes exhibit the variation. This is unlike the Procrustes method where you can have two points differ significantly from the mean between strains and not necessarily indicate there is localized effect. This is because a variation in one landmark can be diluted across all landmarks, a consistent criticism of the least-squares Procrustes superimposition method. The reason for this lies in the

fact that the distance from any particular landmark to the mean depends on all other points within that sample. We believe that the localization potential of TBM will be especially valuable when it comes to identifying areas for genetic evaluation.

Results from the longitudinal sample were able to isolate areas of distinct change in the developing mandible. (Figure 32) Additionally, it should be noted that these findings are temporally consistent with previous studies that also found mandibular shape shows significant development until approximately 60 days, after which it tapers off considerably.[50] We also show that there was no real significant change after such time, suggesting that mandibular shape, at least in this particular strain, reaches maturity somewhere between 60 and 90 days. Lastly, the results from this longitudinal sample suggest that mandibular shape does not develop in a uniform fashion, but rather there exist particular areas of more intense growth than others. This interpretation supplements the current literature describing the modularity of skeletal growth and findings that the mandible develops from different mesenchymal condensations.[13,51,52]

Finally, we hope that the results of this exploratory study illustrate the strength of tensor-based morphometric techniques to capture the multidimensionality of mandibular shape and allow us to obtain quantitative shape comparisons that can be easily visualized by the observer. To further illustrate an immediate application of these results, per findings described in Figure 33, our lab was able to dissect a 14-day old mandible and extract quality RNA from these regions. (Figure 34, Figure 35)

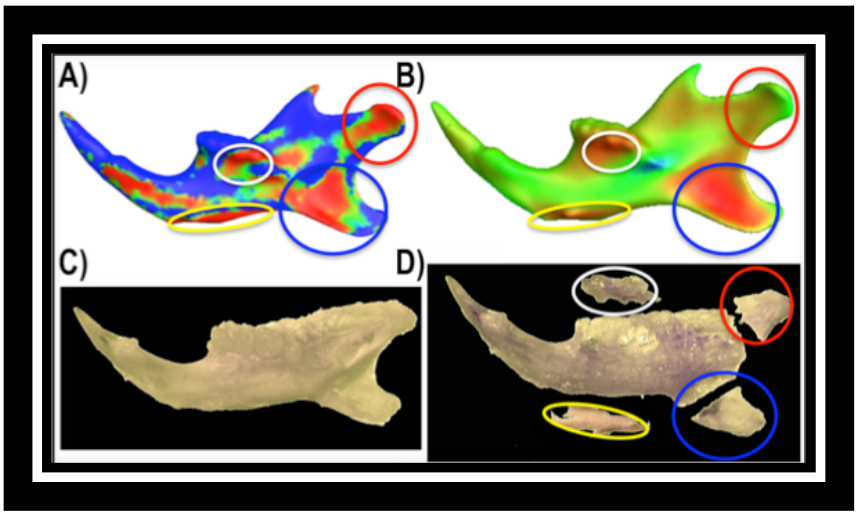

Figure 34: Significant areas of interstrain (A) and developmental (B) shape variation isolated and dissected for RNA extraction (C), (D).

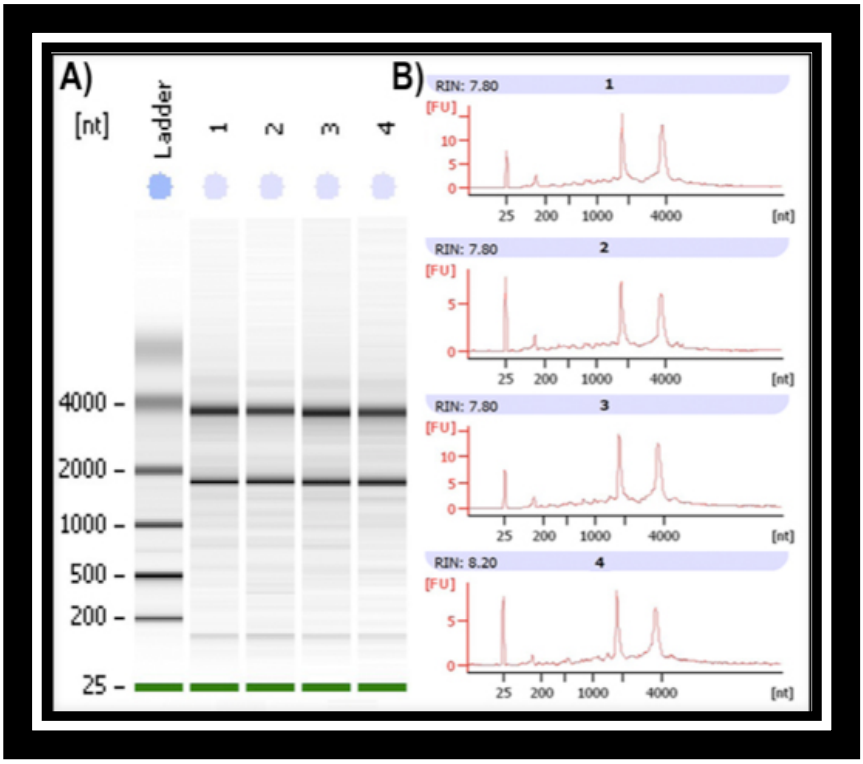

Figure 35: Gel electrophoresis (A) and RIN values (B) from each of the isolated areas.

Limitations and Alternatives:

We recognize that our population sample was small, however, the purpose of this study is more a proof of principle and methodloigcal development. While this methodology offers an original approach for analyzing the mouse mandible, it is not without its limitations. One of the most basic limitations lies with one of the initial steps of setting the threshold within Dolphin Imaging®. Despite the fact we set a protocol in an attempt to standardize the threshold, the setting was based on a sliding toggle. As mentioned, we aimed to minimize both noise and pseudofenestrations, however this step may have introduced some degree of error into our data. It is possible that this step may be improved with numerical assignment to the threshold buttons in an effort to quantify the threshold setting, or by utilizing alternative software to create the surfaces from the volumetric datasets.

As for tensor-based morphometry, we acknowledge that TBM will not isolate overall changes in congruent shape transformation. For example, because TBM is a local technique it will not register the gross bending of a particular shape without either enlargement or shrinkage. This limitation, however, can be overcome by coupling TBM with either the medial axis technique or landmark-free Procrustes analysis. Landmark-free Procrustes was also explored in this study but not included in order to limit content. The premise is similar to landmark-based Procrustes superimposition except that the points are developed from the vertices on the shape's surface rather than points placed manually.[55] Medial axis analysis is advantageous to the Procrustes approach in the sense that each computed axis is a property of that particular shape and does not rely on comparison to a reference shape or other landmarks. It offers an additional geometric morphometric technique that lies in between intrinsic shape properties and the ability

to co-localize shape variation. Moreover, the medial thickness of an object is easy to interpret, as it is literally how far a point on the surface of an object lies from the computed medial axis. Either of these methods should possibly be employed to supplement shape analysis and elucidate and variations in shape that may not be captured by TBM.

Conclusions:

1. Based on previous literature, this study has generated the necessary tools to isolate the surface of the mouse mandible and generate a population average to utilize in comparing variations in shape.
2. Through implementation of neuroimaging techniques, primarily TBM and medial axis, both a cross-sectional interstrain sample and longitudinal intrastrain sample were successfully compared and distinct areas of significant shape variation were identified. Notably, the identified regions both coincided with each other and subsequently withstood heritability tests.
3. Areas of significant shape variation within the mandible of the five parental strains examined include the condyle, the angle, the inferior border and the alveolar process housing the molars.
4. "P-maps" offer a visually intuitive model for describing the results found using the methods contained within this study.
5. Tensor-based morphometric evaluation of mandibular shape has far superior visualization and localization potential when compared to the current method using landmark-based analysis, while offering a more reliable solution as it eliminates the need for consistent landmark placement.

6. Further research efforts will focus on characterizing the genetic determinants of mandibular shape using the entire Hybrid Mouse Diversity Panel, as well as developing the protocol to adapt to other craniofacial structures.

Bibliography:

1. Adams DC, Rohlf FJ, Slice DE. Geometric morphometrics: Ten years of progress following the "revolution." *Ital J Zool*. 2004;71(1):5–16. doi:10.1080/11250000409356545.

2. Bumpus HC. The elimination of the unfit as illustrated by the introduced sparrow Passer domesticus. *Biol Lect Biol Lab,*. 1898:206–209.

3. Loy A. Morphometrics and theriology homage to Marco Corti. *Hystrix, Ital J Mammal*. 2007;18(2):115–136.

4. Holland E. Limitations of traditional morphometrics in research on the attractiveness of faces. *Psychon Bull Rev*. 2009;16(3):613–5. doi:10.3758/PBR.16.3.613.

5. Jungers WL, Falsetti AB, Wall CE. Shape, relative size, and size-adjustments in morphometrics. *Am J Phys Anthropol*. 1995;38(S21):137–161. doi:10.1002/ajpa.1330380608.

6. Rohlf FJ, Marcus LF. A Revolution in Morphometrics. 1993;8(4):129–132.

7. Klingenberg CP. Visualizations in geometric morphometrics : how to read and how to make graphs showing shape changes Shape and shape changes : two key concepts in geometric morphometrics. *Hystrix, Ital J Mammal*. 2013;24(May):1–10. doi:10.4404/hystrix-24.1-7691.

8. Drake AG, Klingenberg CP. Large-scale diversification of skull shape in domestic dogs: disparity and modularity. *Am Nat*. 2010;175(3):289–301. doi:10.1086/650372.

9. Atchley WR, Hall BK. A model for development and evolution of complex morphological structures. *Biol Rev Camb Philos Soc*. 1991;66(2):101–57. Available at: http://www.ncbi.nlm.nih.gov/pubmed/1863686.

10. Klingenberg CP, Mebus K, Auffray J-C. Developmental integration in a complex morphological structure: how distinct are the modules in the mouse mandible? *Evol Dev*. 2003;5(5):522–31. Available at: http://www.ncbi.nlm.nih.gov/pubmed/12950630.

11. Klingenberg CP. Morphometric integration and modularity in configurations of landmarks: tools for evaluating a priori hypotheses. *Evol Dev*. 2009;11(4):405–21. doi:10.1111/j.1525-142X.2009.00347.x.

12. Leamy LJ, Klingenberg CP, Sherratt E, Wolf JB, Cheverud JM. A search for quantitative trait loci exhibiting imprinting effects on mouse mandible size and shape. *Heredity (Edinb)*. 2008;101(6):518–526. doi:10.1038/hdy.2008.79.

13. Zelditch ML, Wood AR, Bonett RM, Swiderski DL. Modularity of the rodent mandible: integrating bones, muscles, and teeth. *Evol Dev*. 2008;10(6):756–68. doi:10.1111/j.1525-142X.2008.00290.x.

14. Boell L, Tautz D. Micro-evolutionary divergence patterns of mandible shapes in wild house mouse (Mus musculus) populations. *BMC Evol Biol*. 2011;11(1):306. doi:10.1186/1471-2148-11-306.

15. Boell L. Lines of least resistance and genetic architecture of house mouse (Mus musculus) mandible shape. *Evol Dev*. 2013;15(3):197–204. doi:10.1111/ede.12033.

16. Willmore KE, Roseman CC, Rogers J, Cheverud JM, Richtsmeier JT. Comparison of Mandibular Phenotypic and Genetic Integration between Baboon and Mouse. *Evol Biol*. 2009;36(1):19–36. doi:10.1007/s11692-009-9056-9.

17. Ragheb H, Thacker N a, Bromiley P a, Tautz D, Schunke AC. Quantitative shape analysis with weighted covariance estimates for increased statistical efficiency. *Front Zool*. 2013;10(1):16. Available at: http://www.pubmedcentral.nih.gov/articlerender.fcgi?artid=3684533&tool=pmcentrez&rendertype=abstract.

18. Bennett BJ, Farber CR, Orozco L, et al. A high-resolution association mapping panel for the dissection of complex traits in mice. *Genome Res*. 2010;20(2):281–90. doi:10.1101/gr.099234.109.

19. McComb RW. An Exploratory Approach for Mapping the Surface of the Human Skull in Three Dimensions: Technical Methods and Clinical Application. 2012:1–56.

20. Schunke AC, Bromiley P a, Tautz D, Thacker N a. TINA manual landmarking tool: software for the precise digitization of 3D landmarks. *Front Zool*. 2012;9(1):6. doi:10.1186/1742-9994-9-6.

21. Klingenberg CP, Barluenga M, Meyer A. SHAPE ANALYSIS OF SYMMETRIC STRUCTURES : QUANTIFYING VARIATION AMONG INDIVIDUALS AND ASYMMETRY SHAPE ANALYSIS OF SYMMETRIC STRUCTURES : QUANTIFYING VARIATION AMONG INDIVIDUALS AND ASYMMETRY. 2002;56(10):1909–1920.

22. Klingenberg CP. Developmental instability as a research tool : using patterns of fluctuating asymmetry to infer the developmental origins of morphological integration. In: *Developmental instability: causes and consequences*. M. Polak. New York, Oxford University Press.; 2003:442–447.

23. Ju T, Zhou Q-Y, Hu S-M. Editing the topology of 3D models by sketching. *ACM Trans Graph*. 2007;26(3):42. doi:10.1145/1276377.1276430.

24. Chaudhari A. Improving Signal to Noise Ratio of Low-Dose CT Image Using Wavelet Transform. *Int J Comput Sci Eng*. 2012;4(05):779–787.

25. Han X, Member S, Xu C, Prince JL, Member S. A Topology Preserving Level Set Method for Geometric Deformable Models. 2003;25(6):755–768.

26. http://www.loni.ucla.edu/twiki/bin/view/CCB/SignedDistance2Mesh. Available at: http://www.loni.ucla.edu/twiki/bin/view/CCB/SignedDistance2Mesh.

27. Friedel I, Schröder P, Desbrun M. Unconstrained spherical parameterization. *ACM SIGGRAPH 2005 Sketches - SIGGRAPH '05*. 2005:134. doi:10.1145/1187112.1187274.

28. Thompson PM, Giedd JN, Woods RP, MacDonald D, Evans a C, Toga a W. Growth patterns in the developing brain detected by using continuum mechanical tensor maps. *Nature*. 2000;404(6774):190–3. doi:10.1038/35004593.

29. Thompson PM, Woods RP, Mega MS, Toga a W. Mathematical/computational challenges in creating deformable and probabilistic atlases of the human brain. *Hum Brain Mapp*. 2000;9(2):81–92. Available at: http://www.ncbi.nlm.nih.gov/pubmed/10680765.

30. Wang Y, Song Y, Rajagopalan P, et al. Surface-based TBM boosts power to detect disease effects on the brain: an N=804 ADNI study. *Neuroimage*. 2011;56(4):1993–2010. doi:10.1016/j.neuroimage.2011.03.040.

31. Gutman B a., Wang Y, Rajagopalan P, Toga AW, Thompson PM. Shape matching with medial curves and 1-D group-wise registration. *2012 9th IEEE Int Symp Biomed Imaging*. 2012:716–719. doi:10.1109/ISBI.2012.6235648.

32. Shi, Y, et al. Inverseconsistent surface mapping with LaplaceBeltrami eigenfeatures. *Process Med Imaging*. 21:467–478.

33. Christensen GE, Rabbitt RD, Miller MI. Deformable templates using large deformation kinematics. *IEEE Trans Image Process*. 1996;5(10):1435–47. doi:10.1109/83.536892.

34. D'Agostino E, Maes F, Vandermeulen D, Suetens P. A viscous fluid model for multimodal non-rigid image registration using mutual information. *Med Image Anal*. 2003;7(4):565–75. Available at: http://www.ncbi.nlm.nih.gov/pubmed/14561559.

35. Hua X, Gutman B, Boyle CP, et al. Accurate measurement of brain changes in longitudinal MRI scans using tensor-based morphometry. *Neuroimage*. 2011;57(1):5–14. doi:10.1016/j.neuroimage.2011.01.079.

36. Shi J, Thompson PM, Gutman B, Wang Y. Surface fluid registration of conformal representation: application to detect disease burden and genetic influence on hippocampus. *Neuroimage*. 2013;78:111–34. doi:10.1016/j.neuroimage.2013.04.018.

37. Gutman BA, Madsen SK, Toga AW, Thompson PM. A Family of Fast Spherical Registration Algorithms for Cortical Shapes. 2013:246–257.

38. Liu L, Chambers W, Letscher D. Extended Grassfire Transform on Medial Axes of 2D Shapes. 2011;(June).

39. Mohideen F, Rodrigo R. Curvature Based Robust Descriptors. *Procedings Br Mach Vis Conf 2012*. 2012:41.1–41.11. doi:10.5244/C.26.41.

40. Tanaka HT, Ikeda M, Chiaki H. Curvature-based face surface recognition using spherical correlation. Principal directions for curved object recognition. *Proc Third IEEE Int Conf Autom Face Gesture Recognit*. 1998:372–377. doi:10.1109/AFGR.1998.670977.

41. Mérigot Q, Sophia-antipolis I, Guibas L. Robust Voronoi-based Curvature and Feature Estimation Categories and Subject Descriptors.

42. Tameem HZ, Ardekani S, Seeger L, Thompson P, Sinha US. Initial results on development and application of statistical atlas of femoral cartilage in osteoarthritis to determine sex differences in structure: data from the Osteoarthritis Initiative. *J Magn Reson Imaging*. 2011;34(2):372–83. doi:10.1002/jmri.22643.

43. Liu F, van der Lijn F, Schurmann C, et al. A genome-wide association study identifies five loci influencing facial morphology in Europeans. *PLoS Genet*. 2012;8(9):e1002932. doi:10.1371/journal.pgen.1002932.

44. Wang Y, Lui LM, Gu X, et al. Riemann Surface Structure. 2007;26(6):853–865.

45. Wang Y, Gu X, Hayashi KM, Chan TF, Thompson PM, Yau S-T. Brain surface parameterization using Riemann surface structure. *Med Image Comput Comput Assist Interv*. 2005;8(Pt 2):657–65. Available at: http://www.ncbi.nlm.nih.gov/pubmed/16686016.

46. Hua X, Leow AD, Lee S, et al. 3D characterization of brain atrophy in Alzheimer's disease and mild cognitive impairment using tensor-based morphometry. *Neuroimage*. 2008;41(1):19–34. doi:10.1016/j.neuroimage.2008.02.010.

47. Ashburner J, Friston KJ. Voxel-based morphometry--the methods. *Neuroimage*. 2000;11(6 Pt 1):805–21. doi:10.1006/nimg.2000.0582.

48. Wang Y, Yuan L, Shi J, et al. Applying tensor-based morphometry to parametric surfaces can improve MRI-based disease diagnosis. *Neuroimage*. 2013;74:209–30. doi:10.1016/j.neuroimage.2013.02.011.

49. Leamy LJ, Klingenberg CP, Sherratt E, Wolf JB, Cheverud JM. A search for quantitative trait loci exhibiting imprinting effects on mouse mandible size and shape. *Heredity (Edinb)*. 2008;101(6):518–26. doi:10.1038/hdy.2008.79.

50. Boell L, Pallares LF, Brodski C, et al. Exploring the effects of gene dosage on mandible shape in mice as a model for studying the genetic basis of natural variation. *Dev Genes Evol*. 2013;223(5):279–87. doi:10.1007/s00427-013-0443-y.

51. Klingenberg CP, Leamy LJ, Cheverud JM. Integration and modularity of quantitative trait locus effects on geometric shape in the mouse mandible. *Genetics*. 2004;166(4):1909–1921.

52. Burgio G, Baylac M, Heyer E, Montagutelli X. Exploration of the genetic organization of morphological modularity on the mouse mandible using a set of interspecific recombinant congenic strains between C57BL/6 and mice of the Mus spretus species. *G3 (Bethesda)*. 2012;2(10):1257–68. doi:10.1534/g3.112.003285.

53. Klingenberg CP. MorphoJ: an integrated software package for geometric morphometrics. *Mol Ecol Resour*. 2011;11(2):353–7. doi:10.1111/j.1755-0998.2010.02924.x.

54. Langers DRM, Jansen JF a, Backes WH. Enhanced signal detection in neuroimaging by means of regional control of the global false discovery rate. *Neuroimage*. 2007;38(1):43–56. doi:10.1016/j.neuroimage.2007.07.031.

55. Thompson PM, Hayashi KM, Sowell ER, et al. Mapping cortical change in Alzheimer's disease, brain development, and schizophrenia. *Neuroimage*. 23 Suppl 1:S2–18. doi:10.1016/j.neuroimage.2004.07.071.